

**NATURAL GAS HYDRATES STORAGE PROJECT**

**FINAL REPORT**

1 October 1997 - 31 May 1999

Principal Investigator

R. E. Rogers

March 26, 1999

Contract DE-AC26-97FT33203

**Mississippi State University**

P.O. Box 9595

129 Etheredge-Hardy Road

Mississippi State, MS 39762

This report was prepared as an account of work sponsored by an agency of the United States Government. Neither the United States Government nor any agency thereof, nor any of their employees, makes any warranty, express or implied, or assumes any legal liability of responsibility for the accuracy, completeness, or usefulness of any information, apparatus, product, or process disclosed, or represents that its use would not infringe privately owned rights. Reference herein to any specific commercial product, process, or service by trade name, trademark, manufacturer, or otherwise does not necessarily constitute or imply its endorsement, recommendation, or favoring by the United States Government or any agency thereof. The views and opinions of authors expressed herein do not necessarily state or reflect those of the United States Government or any agency thereof.

## ABSTRACT

Since economical and environmental conditions could be positively affected by greater use of natural gas, especially for peak-loading events of power plants, the feasibility of overcoming a major impediment of safe, aboveground storage in heavily populated areas was sought in the work funded by DE-AC26-97FT33203. Principal deterrent to utilizing natural gas to its fullest is the difficulty of on-site storage; principal incentive to utilizing natural gas to its fullest is its clean-burning quality and its relatively low cost.

Storage of natural gas in gas hydrates would have distinct inherent advantages of safety (stored gas would be essentially encased in ice), slow dissipation of gas in case of tank failure, and low operating pressures.

Greatly improved formation rates, packing density and process simplification were achieved in the subject study by incorporating sodium dodecyl sulfate in water at concentrations above the critical micellar concentration. Natural gas storage capacities of 155 vol-gas/vol-hydrate were demonstrated at 3.89 MPa (565 psia) and 275.4 K (36°F) in a quiescent system in less than 3 hours after hydrate initiation. The surfactant also causes hydrate adsorption and packing on the test-cell walls as the hydrates form. The process was shown to be technically feasible in the laboratory work.

To be feasible economically, a hydrate-storage process must be simple to minimize labor, maintenance, and equipment costs. The process envisioned from the laboratory work appears attractive in its simplicity. Development of design concepts and economic analysis are recommended as the next step.

## TABLE OF CONTENTS

	Page
Abstract .....	i
Table of Contents .....	ii
List of Figures .....	iii
List of Tables .....	iv
Executive Summary .....	v
Introduction .....	1
A. Historical, State-of-the-Art .....	1
B. Structure, Properties of Hydrates .....	2
C. Rate of Hydrate Formation .....	3
D. Formation Mechanism, Quiescent State .....	4
E. Test Apparatus .....	5
F. Test Procedure .....	7
Results and Discussion .....	8
I. Surfactant Effects .....	8
A. Storage Capacity with Surfactant .....	8
(1) Conversion of Interstitial Water in Batch Process .....	9
(2) Conversion of Interstitial Water in Semi-Continuous Process .....	10
(3) Surfactant Improvement of Attainable Storage Capacity .....	10
B. Formation Rates with Surfactant .....	11
(1) Formation Rates in Batch System .....	11
(2) Formation Rates in Semi-Continuous System .....	15
C. Process Simplification and Economy with Surfactant .....	15
(1) Simplification from High Formation Rate .....	16
(2) Simplification from Quiescent System .....	16
(3) Simplification--Cell Wall Buildup .....	16
D. Hydrate Formation Mechanism .....	22
(1) Surfactant alteration of hydrate formation mechanism .....	22
(2) CMC at Hydrate-Forming Conditions .....	24
II. Pressure Effects .....	25
III. Temperature Effects .....	29
IV. Natural Gas Composition Effects .....	30
A. Formation Compositions .....	30
B. Withdrawal Compositions .....	31
V. Decomposition .....	32
A. Hysteresis of Formation/Decomposition .....	32
B. Effect of Total Pressure on Decomposition .....	34
C. Decomposition with Microwaves .....	35
VI. Impact of Study on Hydrate Storage Feasibility .....	40
A. Statement of Process Technical Need and Capability .....	40
B. Hydrate Formation/Storage Tank .....	40
(1) Characteristics to Incorporate .....	40
(2) Sketch of Tank Concept .....	42
VII. Conclusions .....	45
VIII. Recommendations .....	46
Bibliography .....	47
List of Acronyms and Abbreviations .....	49

## LIST OF FIGURES

Fig. 1. Sketch of test apparatus . . . . .	5
Fig. 2. Natural gas storage capacity, batch process . . . . .	9
Fig. 3. Interstitial water conversion at constant high pressure . . . . .	10
Fig. 4. Photograph of ethane packing test cell to maximum loading . . . . .	11
Fig. 5. SDS surfactant increases hydrate formation rate . . . . .	12
Fig. 6. Storage capacity and rate of natural gas hydrates . . . . .	14
Fig. 7. Interstitial water converted at high rate . . . . .	14
Fig. 8. Beginning growth of hydrate crystals--pure water/ethane . . . . .	17
Fig. 9. Developed growth of hydrate crystals--pure water/ethane . . . . .	18
Fig. 10. Beginning growth of hydrate crystals--surfactant/water/ethane . . . . .	19
Fig. 11. Developed growth of hydrate crystals--surfactant/water/ethane . . . . .	20
Fig. 12. Growth of hydrate crystals--surfactant/water/natural gas . . . . .	21
Fig. 13. Model of micelle in hydrate-forming system . . . . .	22
Fig. 14. Observed hydrate formation subsurface with surfactant . . . . .	23
Fig. 15. Critical micellar concentration of SDS, 1 atm . . . . .	24
Fig. 16. Hydrate induction time defines CMC . . . . .	25
Fig. 17. Pressure increases natural gas storage capacity . . . . .	27
Fig. 18. Pressure trends of natural gas storage capacity . . . . .	28
Fig. 19. Gas-phase temperature more sensitive to natural gas hydrate formation . . . . .	29
Fig. 20. Hysteresis of formation/decomposition cycle . . . . .	33
Fig. 21. Photograph of gas bubbles during decomposition . . . . .	34
Fig. 22. Apparatus for microwave injection . . . . .	36
Fig. 23. Microwave response with water in system . . . . .	37
Fig. 24. Hydrate decomposition with cascading microwave pulses . . . . .	38
Fig. 25. Optimum microwave wattage for hydrate decomposition . . . . .	39
Fig. 26. Hydrate formation/storage/decomposition tank . . . . .	42
Fig. 27. Time sequence of hydrate formation in storage tank . . . . .	43
Fig. 28. Concept of hydrate accumulation, storage tank . . . . .	44

## LIST OF TABLES

I. Fraction of small and large cavities filled . . . . .	26
II. Fraction of small and large cavities filled . . . . .	26
III. Summary of occluded and free gas compositions . . . . .	30
IV. Natural gas withdrawal gas compositions . . . . .	32

## EXECUTIVE SUMMARY

Although the unique gas-storage property of hydrates has long been known, their use industrially to store gas has never been utilized. The subject study was made to determine industrial potential of hydrates for gas storage; specifically, the study was to determine the feasibility of gas-hydrate storage for electric power plants to help meet peak-load fuel needs.

A breakthrough was achieved early in the study when the extraordinary effects of surfactant on the process were discovered. Thereafter, efforts centered on developing a surfactant-water based system to form the hydrates.

The surfactant sodium dodecyl sulfate (biodegradable, nontoxic, cheap) in hydrate-forming water concentrations as low as 286 ppm was found to resolve three major processing problems: (1) Hydrate formation rates were increased by a factor of about 700. (2) Hydrate particles formed, adsorbed, and packed on the tank walls--avoiding a technically difficult and economically forbidding mechanical separation and packaging step of removing hydrate particles from a water slurry. (3) Free water trapped between hydrate particles adsorbed on the vessel walls continued to occlude gas to full utilization of free water to provide a maximum packing density. (4) Processing was simplified: forming and storing hydrates in the same tank, reusing water in the storage tank without removing from that vessel, injecting gas and forming hydrates in a quiescent state, separating and packing of storage particles without mechanical assistance.

The presence of propane is necessary for lower-pressure Type II hydrates; both propane and ethane facilitate low-pressure processing. A gas mixture of 90% methane, 6% ethane and 4% propane was used in the experiments as a typical feed-gas composition representing relative amounts of the three hydrocarbons in natural gas. It was determined that 155 vol/vol of natural gas of this composition could be stored in hydrates at 3.89 MPa (550 psig) and 564.9 K (36°F). Or at a lower processing pressure of 3.57 MPa (518.3 psia), 148 vol-gas/vol-hydrate could be stored. Moreover, formation rates are such that 86% of the theoretical maximum storage capacity could be achieved within 2 ½ hours, thus allowing a complete cycle of gas-hydrate formation, decomposition, and turn-around-time within a 24-hour period.

With surfactant, a hydrate storage process becomes technically feasible. The simplicity of the process with surfactant improves the probability of an economically-viable process. Based on the laboratory data, a design concept of a formation/storage tank is presented. It is recommended to develop a final process design and economic study in a follow-on, option phase of this study.

## INTRODUCTION

### A. Historical, State-of-the Art

Gas hydrates were discovered in 1810 by Davy, chlorine gas being occluded in those first hydrates. Although their unique storage capabilities were recognized, they remained a laboratory curiosity. Expanded interest and research developed in about 1940 prompted mainly by hydrates' nuisance in the oil field. Consequently, the thrust of research became to develop means to prevent hydrate occurrence in hydrocarbon transmission lines through arctic regions and subsea. In the 1980s and 1990s discoveries of large quantities of gas stored in naturally-occurring hydrates on the sea floor, perhaps as much as 1116 trillion cubic meters (tcm) of hydrocarbon gases, was a major impetus in the current acceleration of hydrate research. The subject DOE grant is the first serious attempt to utilize the unique properties of hydrates to store natural gas for applications such as peak loads of electric power plants. The objective of this contract DE-AC26-97FT33202 was to determine the technical feasibility of using gas hydrates to store natural gas aboveground for peak loading of electric power plants; if found feasible, a follow-on phase would develop a conceptual design of a large-scale process and would determine the economic viability of such a process.

At the beginning of the current work, November 1997, hydrate state-of-the-art recognized positive and negative factors regarding feasibility of gas storage in hydrates.

The positive factors known at project initiation were the following: (1) 180+ vol-gas/vol-hydrate could be stored. (2) Safety of storing natural gas in hydrates was unmatched, for gas would be essentially encased in ice. (3) Gas could be stored in the hydrates at relatively low pressures. (4) The slow release of gas from hydrates in the event of storage-tank rupture enhances safety. (5) Vast quantities of gas stored in naturally-occurring hydrates were known.

Also, at the beginning of the project, the following negative factors diminished feasibility prospects: (1) The formation of hydrates in a quiescent pure water-hydrocarbon gas was extremely slow at hydrate-forming temperatures and pressures. Historically, hydrate formation in the laboratory with a rocking cell apparatus had been cumbersome and slow. (The rocking motion establishes enough turbulence to periodically sweep away the hydrate film that forms on the water surface preventing contact with the gas.) (2) The state-of-the-art process was complex for scaleup, especially if a mechanically stirred reactor became necessary to achieve acceptable formation rates. (3) The slurry separation and packing of hydrate particles formed in a mechanically-stirred reactor seemed prohibiting. (4) When hydrate particles form, much free water is trapped in the interstices of particles. Therefore, free water between particles would occupy much of the expensive storage tank. (5) A storage process for hydrates had never been demonstrated.

These negative factors had to be overcome to develop a feasible process.

## B. Structure, Properties of Hydrates

Natural gas hydrates are crystalline inclusion compounds formed when natural gas under pressure comes into contact with water at low temperatures. Through hydrogen bonding, the host water molecules form a lattice structure resembling a cage. The hydrate lattices contain large vacancies or cavities. These cavities are at least partially occupied by small gas molecules such as CH<sub>4</sub>, C<sub>2</sub>H<sub>6</sub>, C<sub>3</sub>H<sub>8</sub>, I-C<sub>4</sub>H<sub>10</sub>, n-C<sub>4</sub>H<sub>10</sub>, N<sub>2</sub>, and CO<sub>2</sub> to stabilize the lattice structure. (Sloan, 1991; Tse et al., 1983; Wilcox et al., 1941) Normally, hydrates are formed in one of two types of repeating crystal structures. The basic water configuration from which the two hydrate structures are formed has 12 faces with 5 sides per face. Links between the vertices of this basic configuration result in type I hydrate structure, while structure II is produced by the coupling of the faces (Sloan, 1990). Each unit cell of a hydrate of structure I consists of 46 water molecules which form two small and six large cavities. The unit cell of a hydrate of structure II consists of 16 small and eight large cavities formed by 136 water molecules.

Each of the two hydrate structures, I and II, accommodates two sizes of molecules. In structure I, gases with molecular diameters up to 5.8 Angstroms can fit in the large cavities, while only molecules of diameter less than 5.2 Angstroms can fit in the small cavities or have the option of filling both cavity sizes. A similar arrangement occurs with the structure II hydrate that has cavities of 4.8 Angstroms and 6.9 Angstroms. If gases such as propane are present with 5.8 > diameter # 6.9 Angstroms, then structure II must form to accommodate the larger molecules (Makogon, 1981; Sloan, 1991). Pentane (C<sub>5</sub>H<sub>12</sub>) and heavier hydrocarbons do not form hydrate because of their size (Carson and Katz, 1941).

Generally, the hydrate number  $n$  (ratio of water to gas molecules in the hydrates) is used to express the composition of gas hydrates. The higher the hydrocarbon concentration, the lower the hydrate number  $n$ . For structure I, the lowest hydrate number is 5.75 (7.67 if only the large cavities are filled). For structure II, the minimum hydrate numbers are 5.67 if all cavities are filled or 17.0 if only the large ones are occupied. The packing of gas molecules in a hydrate structure approaches that of liquid form (Makogon, 1981).

The volume of gas stored in a given volume of hydrates under hydrate formation conditions of pressure and temperature is calculated using Eq. (1) (Makogon, 1981).

$$V_{GH} = (VnV_G 10^3) / M_h \quad (1)$$

The equation for the molecular weight  $M_h$  of the hydrates reads

$$M_h = M + 18.02 n \quad (2)$$

The hydrate number  $n$  is given by Eqs. (3) and (4) for structures I and II, respectively. (Spontak, 1986; Sloan, 1990)

$$n = 46 / (2\epsilon_{sm} + 6\epsilon_{bg}) \quad (3)$$

or

$$n = 136 / (16\epsilon_{sm} + 8\epsilon_{bg}) \quad (4)$$

A detailed discussion on the determination of the fractional fillings  $\epsilon_{sm}$  and  $\epsilon_{bg}$  of the small and large cavities is given by Makogon (1981) and Sloan (1990).

The density of hydrates formed by gas mixtures is given by Eq. (5) (Makogon, 1981)

$$\tilde{n} = \frac{\sum_j N_j (M_j + 18.02n_j)}{\sum_j 18.02N_j V_j n_j} \quad (5)$$

Where

- $M$  = molecular weight of gas mixture
- $M_h$  = molecular weight of hydrate
- $M_i$  = molecular weight of hydrate forming gas I
- $V$  = volume of hydrate (m<sup>3</sup>)
- $V_{GH}$  = volume of gas stored in hydrate (m<sup>3</sup>)
- $V_i$  = specific volume of water in hydrate formed by component I (m<sup>3</sup>/kg)
- $V_g$  = percentage of volume of gas stored in hydrates, nondimensional
- $n$  = hydrate number, nondimensional
- $\tilde{n}$  = density (kg/m<sup>3</sup>)
- $\epsilon_{bg}, \epsilon_{sm}$  = fractional filling of large and small cavities, nondimensional

### C. Rate of Hydrate Formation

The basic rate equation for hydrate formation relates pressure, temperature, degree of supercooling, and water-gas interface area (Vysniauskas and Bishnoi, 1983). In eq. (6)  $A$  represents a lumped pre-exponential constant,  $a_s$  is the water-gas interfacial area,  $\tilde{A}E_a$  is the activation energy for hydrate formation,  $R$  is the universal gas constant,  $T$  represents absolute temperature,  $P$  represents system pressure,  $a$  and  $b$  are arbitrary constants and  $\tilde{a}$  is the overall order of reaction with respect to pressure.

$$r = A a_s \exp\left(-\frac{\ddot{A}E_a}{RT}\right) \exp\left(-\frac{a}{\ddot{A}T^b}\right) P^{\ddot{a}} \quad (6)$$

The parameters in the equation have been established for a methane-pure water system (Vysniauskas and Bishnoi, 1983) and ethane-pure water system (Vysniauskas and Bishnoi, 1985) in which the water was mechanically stirred. It is useful to keep in mind eq. (6) as the effects of surfactants on the rate of formation are discussed.

The interfacial area between the liquid water and gas is generally established in laboratory experimentation by vigorously agitating the test cell contents as hydrates form, continually regenerating the contact surface of gas and water. For example, in the experimental apparatus of Narita (1996) an impeller speed of 500 rpm gave a maximum hydrate reaction rate. At 500 rpm, Vysniauskas and Bishnoi (1983) estimated a surface area of the gas/water interface as 106 cm<sup>2</sup> for their system. For rapid hydrate formation, a renewable surface is necessary because a thin film of hydrates which forms on the water surface isolates the gas from the water to decrease gas absorption rate into the free water (Herri *et al.*, 1996). Therefore, hydrate formation rate in a quiescent system is extremely slow and controlled by the diffusion rate of the gas as well as the water through the thin hydrate film (Mori and Mochizuk, 1996).

A latent heat of formation of about 65.4 kJ/mol (Sloan, 1990) is released at the water-gas interface when hydrates form, introducing heat transfer rate as a factor in hydrate formation rate as it affects the temperature terms in eq. (6). The relatively large release of heat creates an experimental problem of determining a true interfacial temperature. Stainless steel surfaces increase formation rates by their conductive removal of heat from the interface and facilitate hydrate formation by being a promoter of nucleation.

#### D. Formation Mechanism, Quiescent State

The mechanism of hydrate formation in a quiescent pure water-gas system is that water molecules first form clusters by hydrogen bonding in the liquid phase, proceeding to cluster and occlude gas until a critical concentration and size of the clusters is reached which is the critical nuclei for hydrate formation (Vysniauskas and Bishnoi, 1983). After an induction time of 20 minutes or less, depending on system conditions, particle agglomeration of these nuclei proceeds at the water-gas interface, resulting in a thin film of hydrates on the surface that isolates the liquid from the gas, drastically slowing the rate of formation. Gas and water then must diffuse through the thin film to perpetuate crystal growth.

In the mechanism of hydrate formation in a quiescent system, free water is trapped between solid hydrate particles. This water may represent a large percentage of the hydrate volume. Englezos (1996) found only 1.4% to 14% of the water in an experimental cell (based on maximum amount that could form hydrates and dependent on the guest molecular identity) was bound in the hydrate structure while

most of the water was trapped between solid particles. The entrapment has been a deterrent to practical use of the hydrates. For example, if gas storage in hydrates for industrial use were the goal, appreciable volumes of the storage tank would be occupied by the trapped water, decreasing storage capacity and rendering hydrates as a gas storage means impractical.

### E. Test Apparatus

The experimental apparatus used in the subject grant is sketched in Fig. 1.

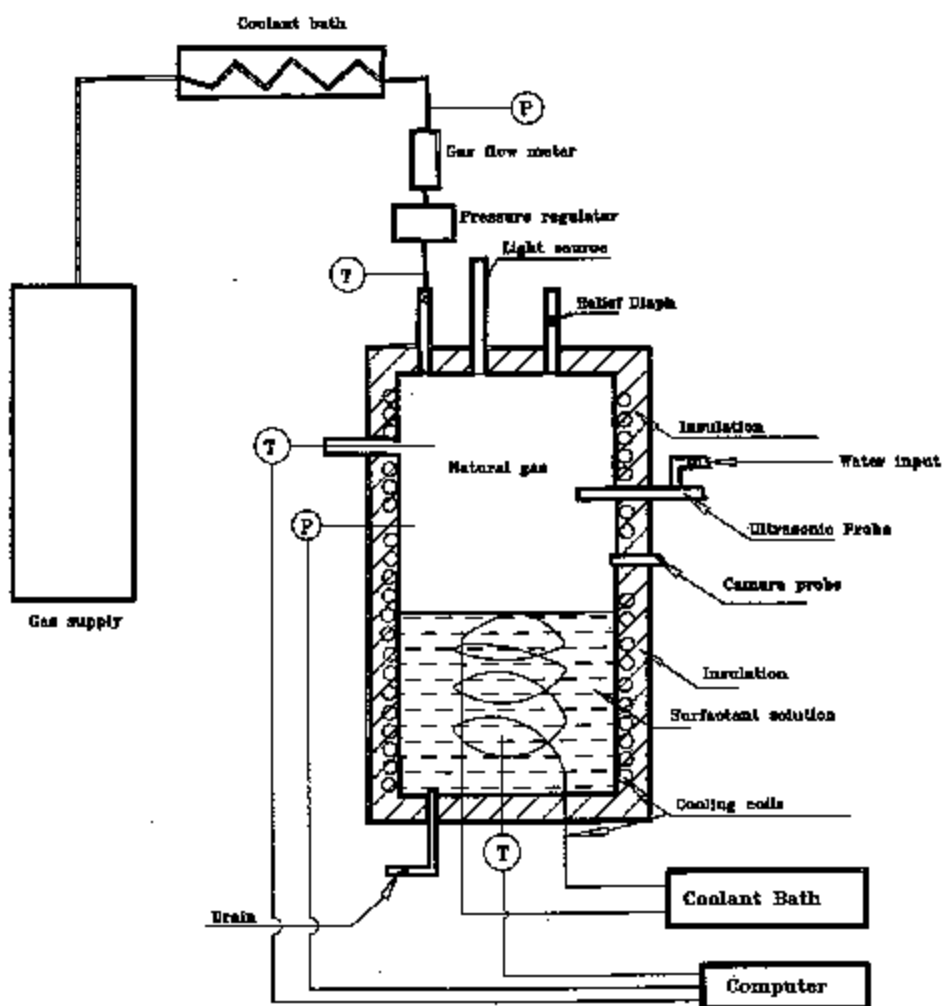


Fig. 1. Sketch of test apparatus.

The 304 stainless steel test cell has a capacity of 3800 cm<sup>3</sup>. Both ends are sealed with blank flanges bolted to the cell; the flanges have phonographic serrated raised faces with 0.79 mm concentric grooves to accommodate sealing with 2.4 mm thick Teflon gaskets. Each blank flange has appropriate ports for access to the interior; additional ports exist along the sides of the cell. Inside the lower half of the cell is a coil of 9.5 mm diameter 316 ss tubing through which is circulated cooling water with enough ethylene glycol to depress the water's freezing point to 253 K. The coolant is circulated from a refrigerated bath capable of maintaining bath temperature within  $\pm 0.01$  K of the set point to a low temperature capability of 253 K. Around the exterior of the cell is also coiled 9.5 mm diameter stainless steel tubing through which the coolant is circulated. The cell and cooling coils are enclosed with insulation. An ultrasonic probe and atomizer extend into the cell from a side port. One RTD probe extends into the bottom of the cell; a second RTD probe extends into the gas phase at the top. One pressure transducer extends into the cell from a side port, and a second transducer monitors pressure in the feed reservoir vessel. A piston metering pump with a maximum pressure capability of 5.52 MPa and a flow rate of 31 ml/min allows metering water solutions into the cell under pressure.

The cell interior is viewed during operation in one of two ways. One choice is to view the interior or take still camera photographs through a 101.6 mm diameter x 50.8 mm thick quartz window secured in a blind flange bolted onto the top of the cell. A second choice is that depicted in Fig. 1. Two 9.5 mm i.d. viewing wells extend into the cell from the top and side of the cell. One well allows light input from a 150 watt halogen light source transmitted by fiber optics light guide. The wells are sealed with transparent sapphire windows pressure checked to 16 MPa. The second well accommodates a Model 702-023K black and white video camera with the image transmitted to either a video cassette recorder for taping and a television monitor for viewing while running or directly to the computer for digital processing. The viewing system was supplied by Instrument Technology, Inc.

A Model FMA-8508 mass gas flowmeter from Omega Engineering, Inc. was used to measure gas added to the cell during hydrate formation. The flowmeter has a capability of 0-5000 sccm, at an accuracy within 1% of full scale and a repeatability of within 0.25% of flow rate. A Tescom Corporation model 26-1026 constant pressure regulator can maintain constant pressure in the cell within  $\pm 6.9$  kPa.

Outputs from the mass flowmeter, RTDs and pressure transducers are recorded and displayed on computer by Omega software and an Omega data acquisition system.

Double-distilled water was used in all experiments. Sodium dodecyl sulfate (SDS), molecular weight of 288.4 g/mole, was purchased from Strem Chemicals, Inc. SDS in powder form was 98%+ pure with no alcohols in the residuals. Surfactant was weighed by means of a Model AG 204 Mettler analytical balance and added to the desired volume of water.

Ethane gas was purchased from Matheson Gas Products. Analysis with the gas chromatograph established an ethane purity of 99.6%. A primary gas mixture of methane, ethane and propane was

purchased from Matheson to give representative and relative quantities of these three major hydrate formers of natural gas. The gas mixture contained 90.01% methane, 5.99% ethane and 4.00% propane. Gases were analyzed by means of a Model 6890 Hewlett-Packard gas chromatograph, using a HPPLLOT-Q column and a flame ionization detector. Ethane was used at the lower pressures in the experiments to establish a procedure, and then the natural gas mixture was used in verification and expansion of the data.

#### F. Test Procedure

A typical procedure was as follows. Initially, surfactant-water solution was pumped into the empty cell to displace all gases. The hydrocarbon gas was then injected to displace water to a predetermined water level. For example, the level could be selected to be along the line of sight of the camera probe in which case liquid completely covered the internal cooling coils. With a pressure below where hydrates could form, the system was cooled to 275 K- 278 K. Pressure was then raised to the operating pressure over a 2-3 minute span by flowing precooled gas into the cell; measurement of gas mass admitted was made with the flowmeter. After reaching desired pressures, constant pressure was maintained as hydrates formed. Hydrate formation was followed by the temperatures, pressures, and mass flows continuously displayed and recorded on the computer. During each experimental run, the inside of the cell was observed on a tv monitor and the video recorded with commentary on video tape.

A second procedure was similar except hydrates formed under a decreasing pressure because occluded gas was not being replenished during the process. In this procedure, the constant-pressure regulator and mass flowmeter were not used; gas contents were followed with gas-law calculations.

In comparing the two foregoing procedures, a faster hydrate formation rate and a larger fraction of the crystal cavities filled when the initial high pressure was kept constant throughout the process.

Two procedures were also used in obtaining photographs for the subject report. In one procedure, camera shots were made through the 101.6 mm (4 in.) diameter quartz window on top of the cell. These give excellent views of hydrate crystal development with and without surfactant. Later in the work, the transparent top was replaced with a fiber-optics/camera system that allowed video tape recording of the action inside the cell. Excellent film was obtained on VHS tape. However, transferring part of the film to still photographs for this report proved difficult in maintaining clarity. The best procedure turned out to be photographing the images on the monitor while playing the film; three photographs in the report were thus taken and presented with the reminder that the video tape is clearer. Excellent footage was recorded on tape.

## RESULTS AND DISCUSSION

It is the objective of the study to determine the feasibility of utilizing gas hydrates to store natural gas for industrial use.

### I. Surfactant Effects

At the beginning of the study it was apparent that technical breakthroughs would be necessary in several areas before hydrates could be successfully used to store natural gas in a large-scale process. Those breakthroughs needed were the following: improved packing fraction of gas in the hydrate mass, faster formation rate of the hydrates, means to collect hydrate particles from water slurry, and process simplification.

A breakthrough came with the introduction of small quantities of an anionic surfactant sodium dodecyl sulfate into the water from which hydrates were to be formed. A dramatic improvement was realized in gas packing fraction, formation rate, collection of particles and process simplification.

#### A. Storage Capacity with Surfactant

There are two separate problems in realizing the highest possible storage capacity of gas in hydrates. The first problem is to fill the cavities of the crystal with gas. The second problem is to increase the packing fraction of hydrate particles.

The first problem may be succinctly stated as follows. Ultimate storage capacity of gas in the hydrates is limited by thermodynamics to about 181 vol-gas/vol-hydrate. That is, all cavities in the hydrate are then filled with natural gas components. As pressure of the system increases, the fraction of filled cavities increases. To establish a practical, cost-effective process for hydrate storage of gas, therefore, one must optimize the pressure, since costs of processing and storage increase with pressure. There must be a tradeoff between added costs of higher pressures and the cost benefits of a larger fraction of cavities filled.

The second problem in establishing practical storage capacity results from the entrapment of free water between hydrate particles. The solid mass of frozen hydrates entrap a large amount of water between particles so that the bulk of hydrate mass formed in a vessel, for example, would contain a large volume of water trapped and isolated from contact with gas. In other words, much of the storage space in the tank would be occupied by water not containing gas. The packing fraction of gas in the frozen mass of hydrates could be low even though the cavities in the hydrate crystals of that mass were mostly filled with occluded gas.

The first problem mentioned above will be discussed in another section; it is thermodynamically limited and not affected by surfactant. The second problem will be addressed at this point because the use of surfactant in the water solves that problem.

### (1) Conversion of Interstitial Water in Batch Process

The entrapped water problem was addressed in a series of experimental runs with natural gas (90.01% methane, 5.99% ethane, 4.00% propane) in which pressure was allowed to decline in the test cell as hydrates formed in a batch-type process. The system conditions were a quiescent state, pressure initially at 3.57 Mpa (518.3 psia), temperature at 274.8- 277.6 K (35-40°F), and 286 ppm SDS in double-distilled water. As pressure approached equilibrium from the first batch of gas, free water was drained from the bottom of the cell. Another batch of gas was added to bring the pressure back to 3.57 MPa. Five such additional batch loadings of gas were made, and each loading was returned to 3.57 MPa at its beginning. With this scenario, hydrate particles formed on the first loading with attendant free water trapped between particles. Since the free water in the bottom of the cell had been drained, any hydrates formed in subsequent loadings necessarily originated from water trapped between hydrate particles. A mass balance using the gas laws revealed how much gas went into hydrates for each loading; along with the time measurement during each loading, the rate of formation was also calculated for each loading.

In Fig. 2 is presented data for natural gas that shows the packing fraction of each loading. Note that the last four loadings represented by the lightly-shaded areas were obtained by extrapolating the data, since the experiments were stopped after six loadings. (The moles of gas found to be in the frozen mass divided by the theoretical moles of gas in the frozen mass if all water was converted to hydrates and all cavities filled with gas is referred to as the packing fraction.)

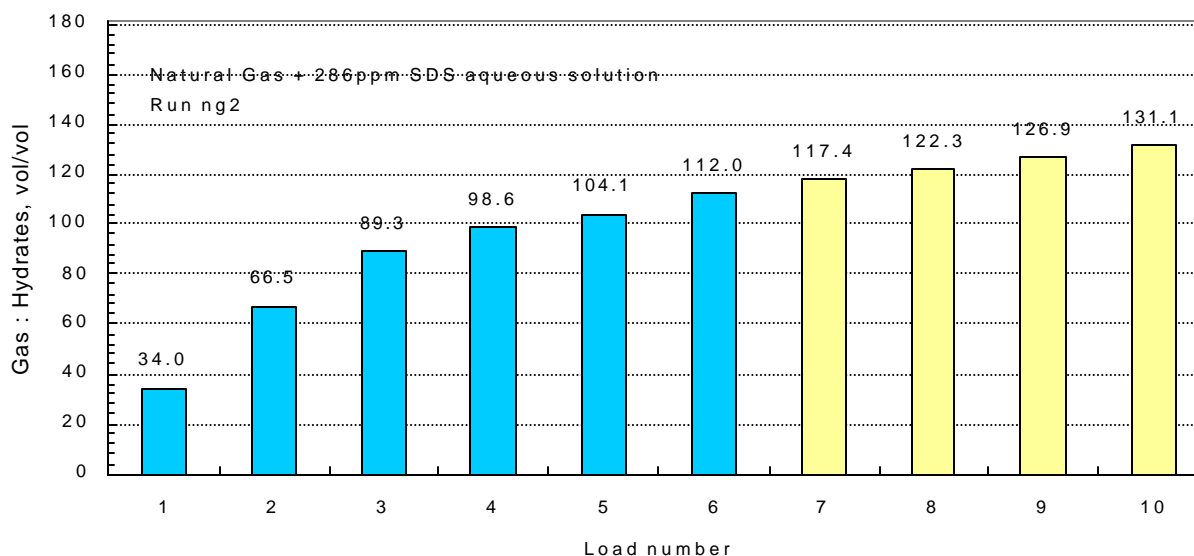


Fig. 2. Natural gas storage capacity, batch process.

To reiterate, the water trapped between particles was converted to hydrates in successive loadings after the free water had been drained from the cell. Our data showed about 62% of maximum packing after the six loadings and about 72% extrapolated to ten loadings for a batch-type process. To achieve a higher packing fraction, therefore, it is advisable to go from a batch process to a semi-continuous process where the maximum gas pressure would be maintained during hydrate formation.

### *(2) Conversion of Interstitial Water in Semi-continuous Process*

The conversion of interstitial water to hydrates was further demonstrated in another experimental run representing a semi-continuous process containing natural gas, water, and 286 ppm SDS. Gas was continuously added to the cell, as needed, to maintain a constant pressure as gas was being occluded during hydrate formation. At the higher constant pressure of a semi-continuous process, a greater fraction of the cavities fill. Natural gas in our test cell was maintained at 3.57 MPa (518.3 psia) with assistance of a constant- pressure regulator; gas added to the cell was measured with a mass flowmeter. All of the free water initially in the bottom of the cell was first converted to hydrates, and then the interstitial water was converted to hydrates. Results showed a 82% achievement of theoretical capacity when processing pressure was maintained at 3.57 MPa. See Fig. 3. At a pressure of 3.89 MPa, 86% of theoretical capacity was achieved. A semi-continuous process would offer a better hope for an economically-viable industrial application.

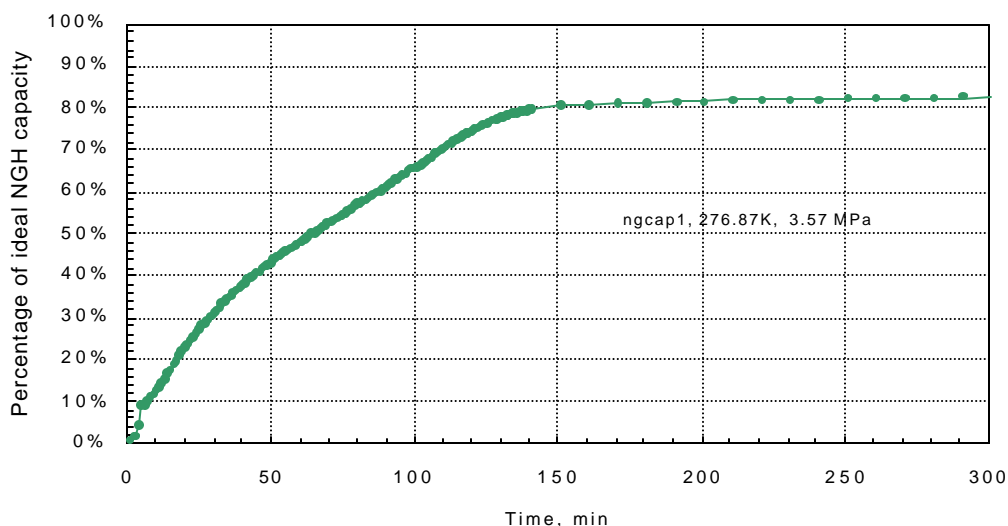


Fig. 3. Interstitial water conversion at constant high pressure.

### *(3) Surfactant Improvement of Attainable Storage Capacity*

Surfactant facilitates the packing of the hydrate particles as they form. The hydrate particles move from the water slurry to the surface of the water because of their buoyancy (specific gravity is less than 1).

Near the water surface, the particles move to the stainless steel walls and are adsorbed on the walls of the container, building inwardly from the walls in a concentric cylinder. Practically, this means that an expensive processing step is avoided of separating particles from a water slurry and packing them in a storage container. Furthermore, space is maximized when the surfactant-laden particles build inwardly from the container walls. Note in the photograph of Fig. 4 taken from the test cell how the hydrates have packed all available space in the cell, leaving a small borehole down the center. In Fig. 4, ethane gas had kept being added to achieve a maximum packing; hydrates filled the cell at the conclusion.

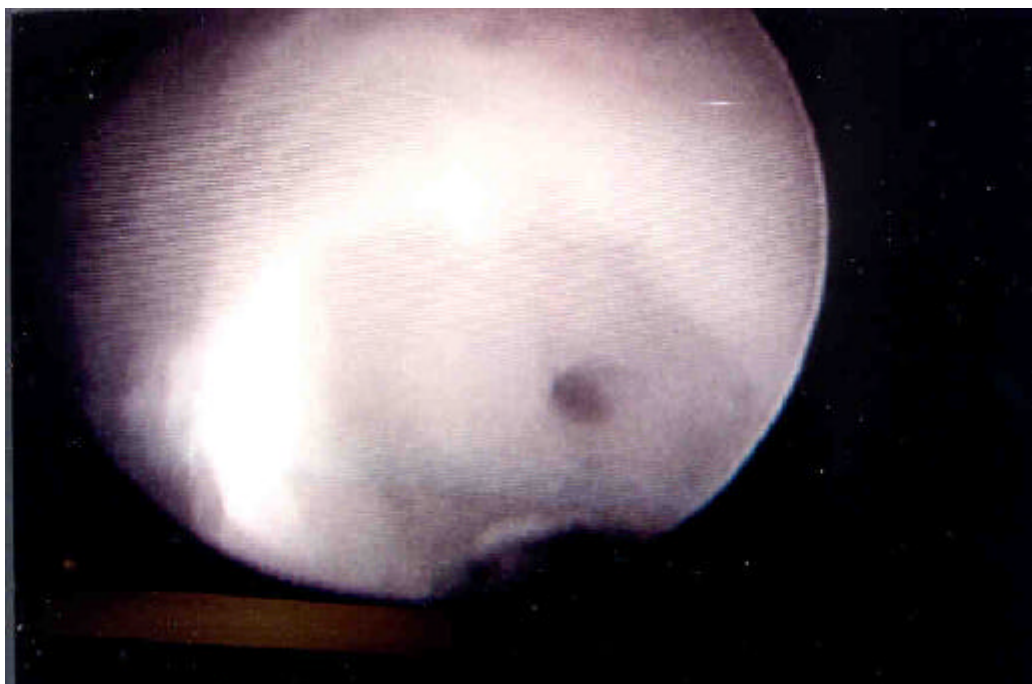


Fig. 4. Photograph of ethane packing test cell to maximum loading.  
(Photographed from VHS film.)

## B. Formation Rate with Surfactant

### *(1) Formation Rates in Batch System*

Hydrates form very slowly in a quiescent system of pure water- hydrocarbon gas. However, the addition of 286 ppm of sodium dodecyl sulfate to the water increases the formation rate in a quiescent system by a factor of about 700. This is evident in Fig. 5 where rate, as represented by the moles of ethane gas occluded per mole of water in our system, is plotted versus time after pressure and temperature had been brought to the hydrate formation conditions.

After about 10 days, the system without surfactant was far from the hydrate capacity reached in less than 3 hours in a 286 ppm SDS surfactant-water system. (Note that the data was taken in a batch system, i.e., gas was not replenished in the cell as pressure declined.) The results are especially striking when the rapidity of hydrate formation in a surfactant system is viewed on the video film which was taken during some experimental runs.

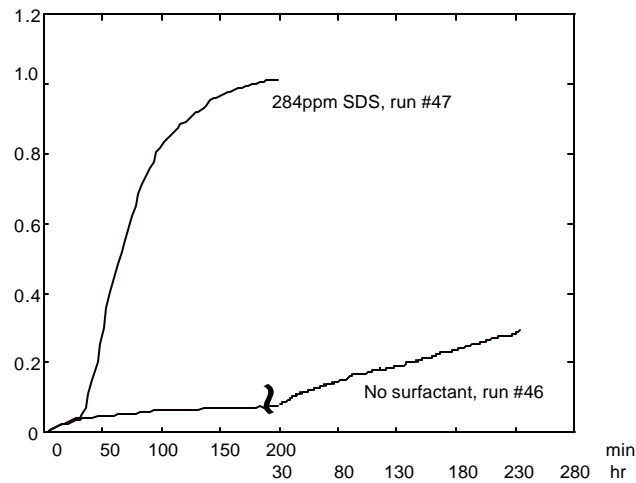


Fig. 5. SDS surfactant increases hydrate formation rate.

As mentioned before and as other researchers have mentioned, free water becomes trapped between hydrate particles upon formation. What is the rate of hydrate formation from the trapped water during each loading and what is the mechanism? The effect of the renewed interfacial surface area between water and gas may be anticipated from Equation 6, which is the rate expression for hydrates forming for a single species of gas or for a gas mixture with a constant composition (Vysniauskas and Bishnoi, 1983).

$$r = A a_s \exp\left(-\frac{\ddot{A}E_a}{RT}\right) \exp\left(-\frac{a}{\ddot{A}T^b}\right) P^{\ddot{a}} \quad (6)$$

Where

A = lumped pre-exponential constant

$a_s$  = water- gas interfacial area

a,b = arbitrary constants

$\ddot{A}E_a$  = activation energy for hydrate formation

P = system pressure

$R$  = universal gas constant

$r$  = rate of hydrocarbon gas consumption during hydrate formation

$T$  = absolute temperature

$\tilde{\alpha}$  = overall order of reaction with respect to pressure

From Equation 6, one expects that increasing the water-gas interfacial area increases the rate of hydrate formation linearly. (Keep in mind that this interfacial area must continually be renewed so that a film of hydrates does not isolate fresh water surface from free gas contact.) With surfactant present, the mechanism is altered, for then discrete particles of hydrates form and surrounding surfactant moves with the particle to adsorb on the vessel walls; water and surfactant are attached to the particle's outer surface. Gas can diffuse through this porous network on the cell walls and thus contact a large surface area of fresh water-surfactant. In summary, surfactant excluded from the hydrate structure concentrates in the trapped water to promote continued hydrate formation as the interstitial water forms hydrates.

Surface tension effects on the formation rate are embodied in the  $A$  term of the equation. The pressure and temperature effects on the formation rate as predicted by eq (6) remain unaltered by surfactants.

A series of experiments was run with natural gas that gives insight into the rate of hydrate formation from the interstitial water. The series involved a batch process, i.e., gas was not continuously replenished to the cell but each gas loading was allowed to approach equilibrium before the next was added. Free water was drained from the bottom of the cell after the first loading of gas so that subsequent hydrate formation occurred from the interstitial water. Temperature was kept constant. With these considerations, view Fig. 6 where rate of formation of natural gas hydrates from interstitial water is superposed on the gas-capacity data of Fig. 2 over the six discrete gas loadings.

Note that the rate of formation of natural gas hydrates increases in going from the first to the second loading but decreases as the interstitial water reacts further even though the interfacial area could be expected to increase. Why?

The following figure illustrates the effect of interstitial water on the formation rate.

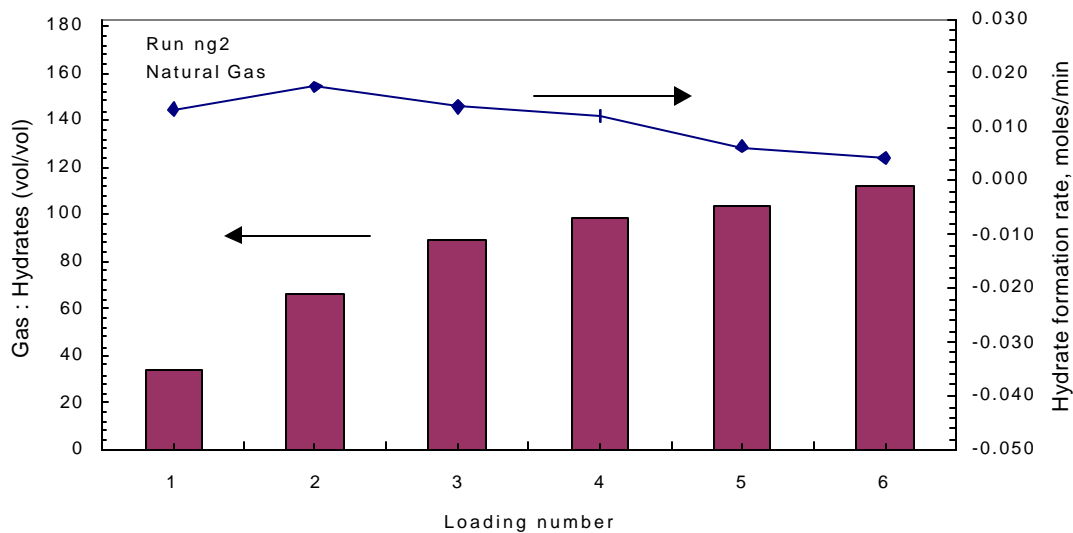


Fig. 6. Storage capacity and rate of natural gas hydrates

To delve into the reason further, consider Fig. 7 in which successive loadings of ethane gas were made rather than successive loadings of a mixture of natural gas.

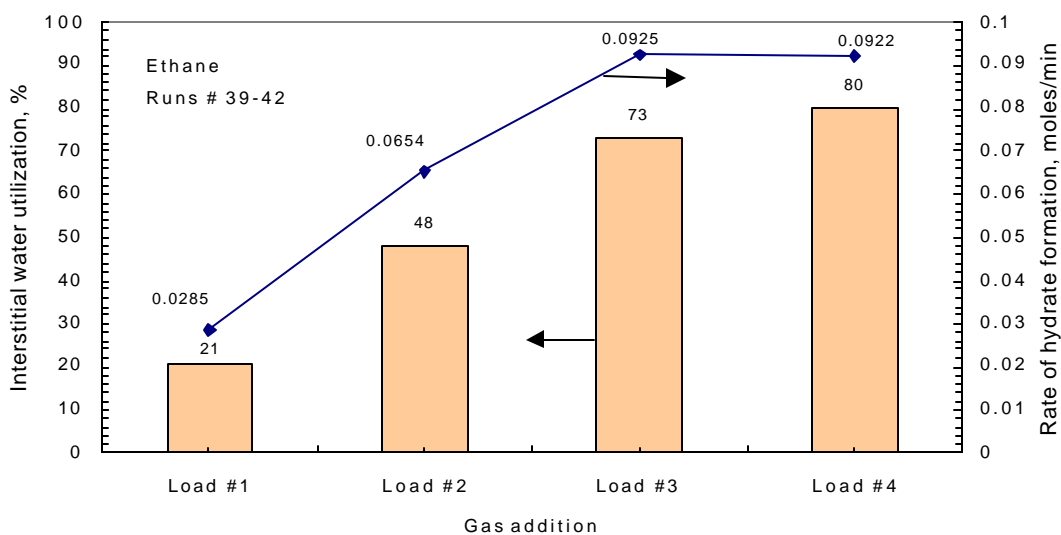


Fig. 7. Interstitial water converted at high rate.

It is seen from Fig. 7 that the rate of formation increases as the interstitial water reacts to form ethane hydrates. When most of the trapped water has reacted (approximately 73%), the formation rate remains constant thereafter. This indicates a lower permeability as interstices become filled with hydrates; mass transfer limits the rate even though interfacial area may be increasing.

It is concluded that three opposing steps determine the rate of hydrate formation from the interstitial water: (1) As more interstitial water is converted, the interfacial area increases between water on the hydrate-particle surfaces and gas, tending to increase the rate.

(2) As more interstitial water is converted, the propane and ethane concentration of the free natural gas decreases, tending to decrease the rate of formation under the falling pressures of this batch process.

(3) As more interstitial water is converted, permeability of the mass of hydrate particles eventually decreases, tending to decrease formation rate.

Therefore, semi-continuous process is suggested by the data for further improvement.

### *(2) Formation Rates in Semi-Continuous System*

The procedure of adding gas to the cell batchwise and then allowing pressure to decline to equilibrium, as presented in Fig. 6 and Fig. 7, results in a lower formation rate and a lower storage capacity than if gas could be continually replenished as hydrates formed to maintain an initial high pressure. In order to verify this, a constant pressure regulator and mass flow meter were installed in the laboratory apparatus. Results from the semi-continuous process were positive and are given later in the report. Such a semi-continuous process is also highly desirable for scale-up of the process.

### C. Process Simplification and Economy with Surfactant

The feasibility of a practical, economical hydrate storage process depends on simplicity. For the sake of simplicity, it would be preferable to have no moving parts in the hydrate formation-storage tank in order to reduce maintenance, labor, operating difficulties, and capital investment. For example, it has been our experience in the laboratory that flow problems abound with hydrates blocking flow lines; this was the case in the beginning of the work upon attempting to spray the water into the gas-pressurized formation tank to create with droplets a large, renewable interface area for faster hydrate formation. Also, serious maintenance and operating problems would arise in a large-scale operation by vigorously stirring the water as hydrates form: How could one provide proper and lasting sealing of the agitator to prevent gas leaks from the pressurized tank? How would one stir the progressively increasing viscosity of the water-hydrate slurry as the solid content increased? How would one pack the hydrate particles formed in an agitated system?

Surfactant in the water solution simplifies the process in three main ways. First, the surfactant causes rapid and complete hydrate formation. Second, the surfactant causes hydrates to form in a

stagnant system. Third, the surfactant attached to hydrates migrate to the cell walls where they are adsorbed and packed.

### *(1) Simplification from High Formation Rate*

In the first simplification, hydrates form rapidly and completely. About 86% of the theoretical limit of gas storage was reached in our test cell within 3 hours of hydrate initiation at 3.89 MPa (564.9 psia) and 275.4 K (36° F). See Fig. 17. This means that with proper design of the formation-storage vessel, a formation-decomposition cycle including turnaround time should be achieved within a 24-hour period. A design concept will be proposed for a process with short turnaround times in the contract option phase.

### *(2) Simplification from Quiescent System*

In the second simplification, surfactant allows the hydrates to be formed in a quiescent system. The alternatives would impose more complex processing steps. One alternative would be to increase water-gas interfacial area by atomizing the water into a pressurized chilled gas to achieve sufficient rate of formation. Another alternative would be to mechanically stir the water-hydrate slurry as hydrates form. Surfactant eliminates the need to impose water flow or moving parts during formation. As a consequence, complexity of the formation/storage tanks would be reduced; in fact, hydrate formation-storage-decomposition would be accomplished in the same vessel. Surfactant would allow reuse of the process water: after decomposition the water and surfactant would remain in the storage tank, and the next formation cycle would proceed by repressurizing with gas. The simplified process greatly enhances the prospects for an economical large-scale process.

### *(3) Simplification--Cell Wall Buildup*

An important simplification from the use of surfactant is that small amounts of SDS in the water cause the hydrate mass to collect on the stainless-steel test cell walls as the hydrate forms. The mechanism will be explained in Section D of *Results and Discussion*. The following photographs emphasize the effect.

The stark difference between a quiescent pure water-gas system and a quiescent water-surfactant-gas system can be seen from photographs taken of the inside of the test cell. First consider hydrates formed in a quiescent system without surfactant in Fig. 8 where the photograph was taken through the transparent quartz top of the pressurized cell. The hydrate crystal growth developed with ethane at 2.41 MPa (350 psi) and 277.6 K (40°F). Note the random growth of the crystals generally extend from one cold metal surface to another, not necessarily associated with the wall surface. The darker mass in the bottom of the cell is free water covered by a sheet of hydrates.

Figure 8 follows.



Fig. 8. Beginning growth of hydrate crystals-pure water/ethane.

In Fig. 9 is the same set of ethane-pure-water crystals 5 days after initiation, still slowly extending their random growth. As the crystals grow, they are trapping free water between particles. Also, as they grow their packing is not such that the space in a storage vessel could be efficiently used. If hydrates were to be utilized in this form to store gas, several processing steps would be necessary to crush and repack the solid-solution mass while maintaining adequate pressure and temperature.

Figure 9 illustrates the slow and random growth of hydrate crystals in a pure water system.



Fig. 9. Developed growth of hydrate crystals--pure water/ethane  
(5 days after hydrate initiation)

However, when sodium dodecyl sulfate is used in water concentrations as low as 286 ppm under similar conditions of pressure and temperature, a different packing occurs in the test cell. Hydrates rapidly grow inwardly from the stainless steel walls of the cell in a concentric cylinder.

As the water level in the cell drops during hydrate formation, the cooling coils become exposed in the bottom of the cell and hydrates then collect around that stainless steel tubing. A photograph taken at the beginning of hydrate formation from a surfactant solution is given in Fig. 10. The photograph was taken only 6.5 minutes after hydrates began to form at a pressure of 2.31 MPa and a temperature near 282 K.

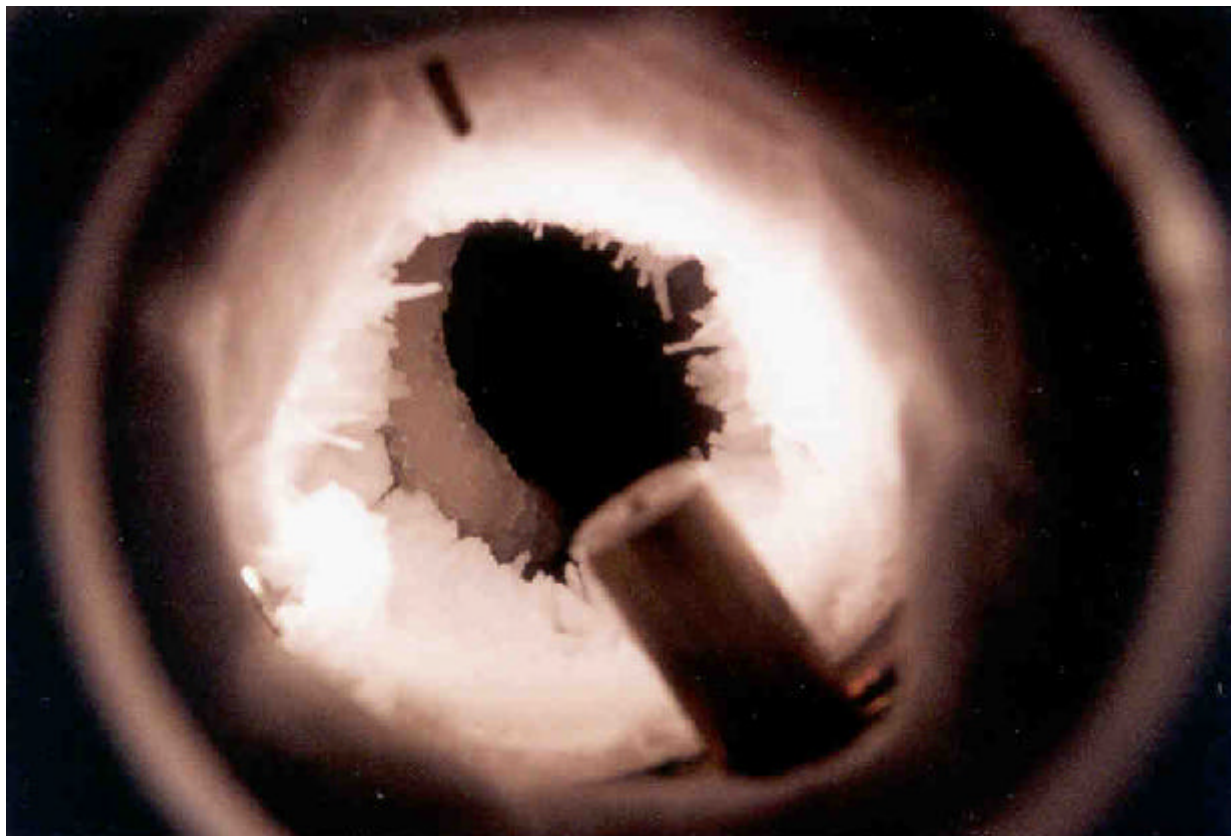


Fig. 10. Beginning growth of hydrate crystals--surfactant/water/ethane.  
(Run #DOE 44)

In Fig. 11 is a photograph of the hydrates formed from a surfactant-water system after much more gas has been occluded. When the free water is depleted in the bottom of the cell, water-surfactant

trapped between hydrate particles on the walls continue forming hydrates.

This hydrate formation from interstitial water increases the bulk density of the hydrate packing, which results in a very efficient packing for storage as can be seen in Fig. 11. The packing appears denser and whiter when compared to Fig. 10, indicating more of the interstitial water has been converted to hydrates. Also, note the stalactite-type protrusions of forming hydrates on the inner surface.



Fig. 11. Developed growth of hydrate crystals--surfactant/water/ethane, Run #34.  
(Some water drops on quartz window are also visible. Taken 3 ½ hours after hydrate initiation.)

The packing arrangement and appearance near ultimate capacity of natural gas in hydrates in our test cell may be viewed in Fig. 12. The photograph was taken after the maximum capacity of natural gas had been loaded into the test cell and occluded in the water-SDS solution. Note that this photograph of near-theoretical-capacity was taken only 3 hours, 57 minutes after hydrate initiation. Also, the solid mass filled the entire cell by growing inwardly from the walls until the cylindrical void in the mass remained slightly off-center; the bottom of the test cell can be seen through the void visible in Fig. 12.

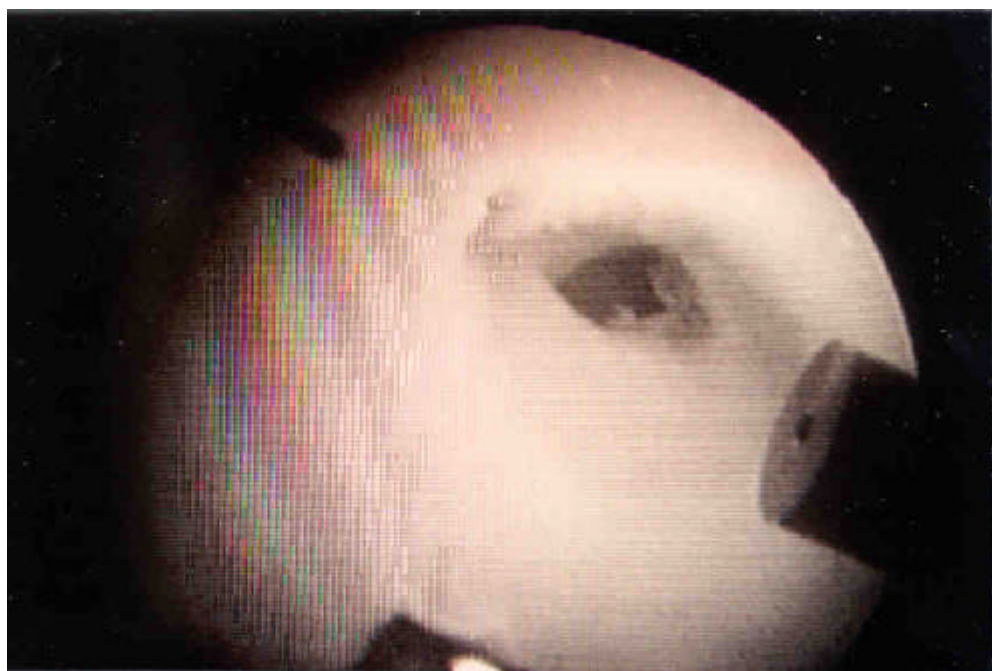


Fig. 12. Growth of hydrate crystals--surfactant/water/natural gas.  
(Photo taken from VHS tape)

The packing arrangement of the hydrate particles formed from the surfactant-water system suggests some cost-effective ways to design a formation-storage tank for natural gas storage in hydrates.

## D. Hydrate Formation Mechanism

### (1) Surfactant Alteration of Hydrate Formation Mechanism

Based on MacKerell's simulation of the SDS micelle configuration (MacKerell, 1995) and our observation of hydrate formation in a water-SDS-ethane system, the micelle model of Fig. 13 for occurrence in a hydrate-forming system is concluded.

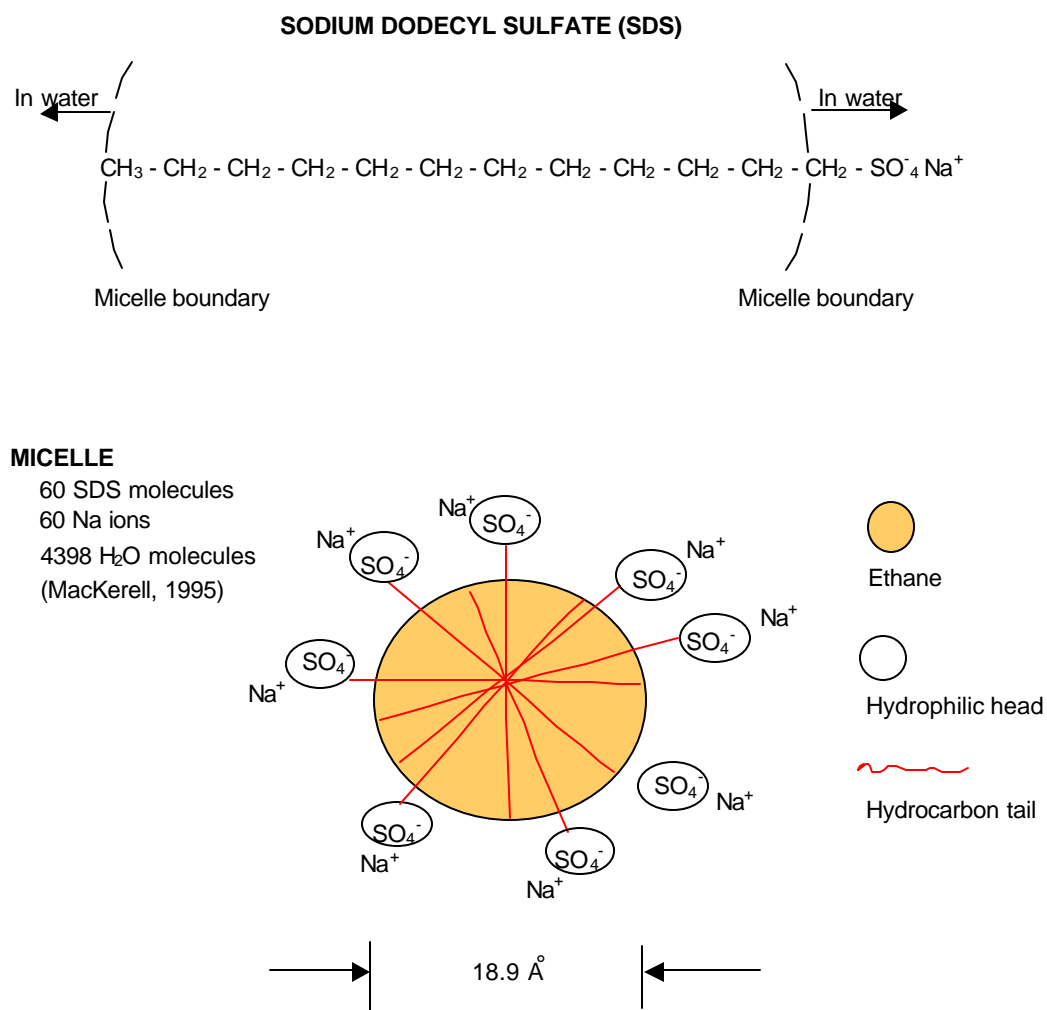


Fig. 13. Model of micelle in hydrate-forming system

Our observations indicate that surfactant micelles facilitate hydrate formation from natural gas

components by concentrating methane, ethane, and propane in the micelle, effectively increasing hydrocarbon solubility in the water; the twelve-carbon tail of the surfactant would solubilize the hydrocarbon gases into the micelle sphere; the proximity to the micelle-water boundary of the terminal methyl groups of SDS helps scavenge the methane, ethane, and propane molecules from the water. Water is excluded from the interior of the micelle sphere where the hydrocarbon gases are concentrated by the saturated hydrocarbon components of SDS. Thus, the gas is brought into intimate contact with the surrounding water, and the micelles act as nucleation sites congregating the water-cluster precursors of hydrates at the surface of the micelle sphere. These sites are located subsurface of the bulk water in the cell as well as on the surface of the bulk water.

In our test cell, hydrate particles were viewed by the fiber optics-camera arrangement and filmed on VHS tape forming below the water surface as depicted in Fig. 14. The camera probe was inserted into the well on the side of the test cell so that the initial water level split the viewing port; one-half of the probe was above water, the other one-half below water. Upon forming subsurface, the particles moved rapidly upward to the water surface and then to the test cell walls. This was a rapid movement of large particle agglomerates.

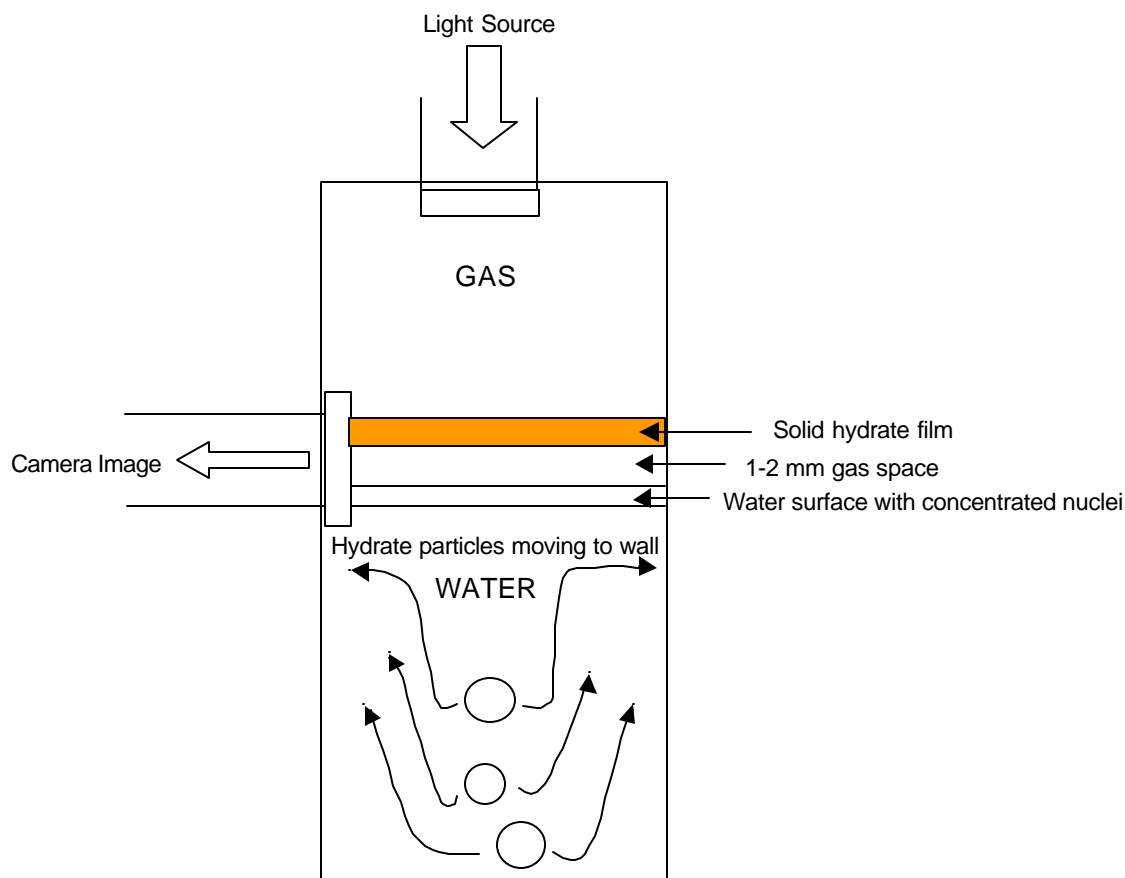


Fig. 14. Observed hydrate formation subsurface with surfactant.

The subsurface hydrate-formation phenomenon in the presence of surfactant is explained by the model of the micelles. The driving force for upward movement of hydrate particles would be buoyancy because hydrate particles are less dense than the water; driving force for their movement to the walls would be their adsorption on that solid surface. Surfactant adsorption at solid-liquid-gas interfaces is common with the micelle structure intact (Wanless and Ducker, 1996). Note that surfactant molecules would be excluded from the hydrate structure, but probably remain oriented at the particle surface and the attraction of surfactant molecules to the stainless-steel surfaces would provide the driving force to move the particles to the walls.

The cylindrical mass buildup of hydrates on the surfactant-wetted, stainless-steel walls continued as water level dropped in the cell.

The boost to gas solubility by micelles and the subsurface migration of the hydrate particles, thereby not creating an obstruction to further hydrate formation, partly account for the 700-fold increase of hydrate formation rate when surfactant is present.

## (2) CMC At Hydrate-Forming Conditions

Critical micellar concentration (CMC) refers to a threshold level of surfactant concentration necessary for micelles to form. Above CMC some physical properties of a solution abruptly change. The sodium dodecyl sulfate (SDS) used in the experimentation was checked for the critical micellar concentration in water. The determination was first made by preparing multiple concentrations of SDS/water solutions and then determining the surface tension at each concentration with a capillary-rise apparatus at ambient temperature and atmospheric pressure. Surface tension is one of the physical properties that sharply changes at the CMC. The results are presented in Fig. 15.

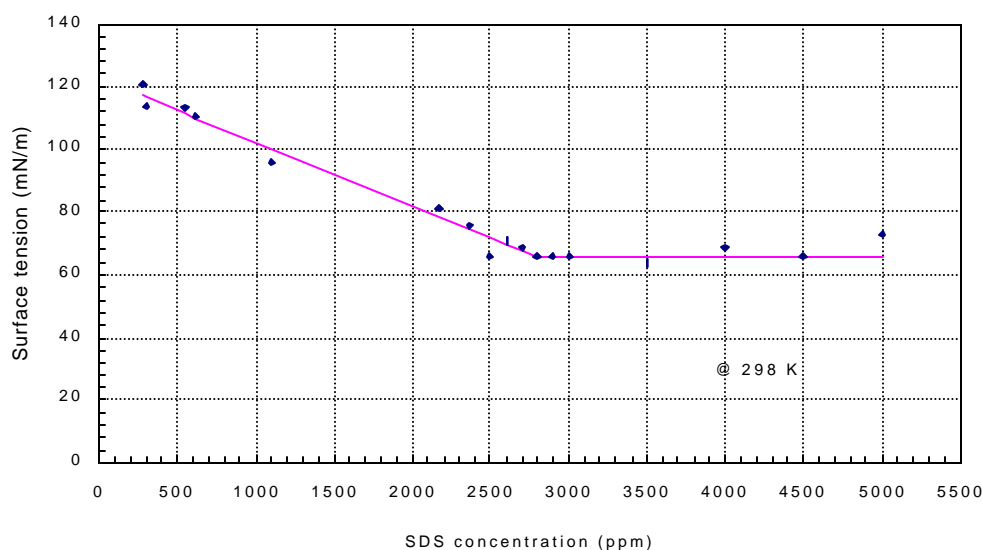


Fig. 15. Critical micellar concentration of sodium dodecyl sulfate, 1 atm.

It is apparent that the CMC at 298 K (77°F) and 1 atm for our solution occurred at 2700 ppm of SDS. However, when using the same surfactant in the chilled and pressurized test cell, hydrates rapidly form at 286 ppm instead of the 2700 ppm. In explanation, CMC is a function of temperature and the amount of gas dissolved in the water (Rosen, 1978). At hydrate-forming conditions the temperature is about 275.4 K (36°F). Gas solubility would be greater at the lower temperature, but hydrocarbon gas solubility increases more rapidly just prior to hydrate formation. Therefore, in order to get a better estimate of CMC at our test conditions, we made multiple runs with ethane in the test cell, varying SDS concentration, attempting to determine the true CMC of the system. The results are given in Fig. 16.

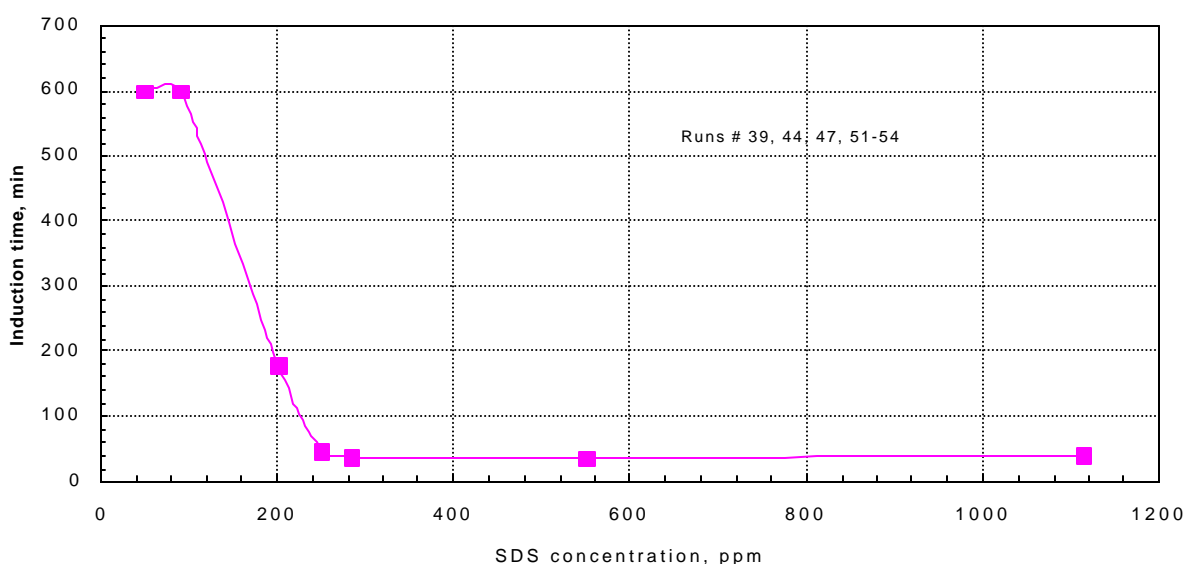


Fig. 16. Hydrate induction time defines CMC.

Note the very sharp break in the curve at 242 ppm, representing the CMC at hydrate-forming conditions for ethane. Induction time gave the most sensitive indication of the breakpoint, although amount of gas occluded at a specific time would also have worked.

The conclusion from Fig. 16 is that a SDS surfactant solution concentration at the CMC of 242 ppm or greater will provide the desired benefits to the hydrate gas-storage process.

## II. Pressure Effects

The storage capacity of natural gas in gas hydrates for large-scale use depends on obtaining a high bulk-density of hydrate particles in the storage vessel and on filling a high fraction of cavities in each individual hydrate crystal. The maximum bulk density can be accomplished with

the addition of surfactant to the water solution, but filling the crystal cavities depends on system pressure.

With our test-gas composition of 90.01% methane, 5.99% ethane and 4.00% propane, the fraction of cavities estimated to be filled as a function of pressure is calculated by the statistical thermodynamics program of Sloan (Sloan, 1992). The results are given in Table I and Table II.

TABLE I. Fraction of small and large cavities filled  
(free gas composition 90.01% CH<sub>4</sub>)

P, MPa	T, K	Percent of small cavity filled			Percent of large cavity filled		
		Methane	Ethane	Propane	Methane	Ethane	Propane
2.86	11.5	0.766027	0	0	0.062497	0.074237	0.858711
3.21	12.4	0.779095	0	0	0.065831	0.075830	0.853912
3.57	13.3	0.790729	0	0	0.069241	0.077395	0.849043

Note: For equilibrium vapor composition: 90.01%, 5.99%, 4%

TABLE II. Fraction of small and large cavities filled  
(free gas composition 99.1% CH<sub>4</sub>)

P, MPa	T, F	Percent of small cavity filled			Percent of large cavity filled		
		Methane	Ethane	Propane	Methane	Ethane	Propane
2.86	2.4	0.834662	0	0	0.617589	0.101905	0.249471
3.21	3.6	0.843456	0	0	0.630381	0.100669	0.239494
3.57	4.5	0.85131	0	0	0.642563	0.099396	0.229982

Note: For equilibrium vapor composition: 99.1%, 0.8%, 0.1%

At a free-gas composition of 90.01% methane, for example, the fraction of small voids filled with methane increases from 76.6% to 79.1% in going from 2.86 MPa (415 psia) to 3.57 MPa (518 psia), while over the same range the large voids remain filled to capacity (99.5%). Therefore, the effect of going to higher pressures is to improve the fractional filling of small cavities with methane.

The amount of natural gas that could be stored in hydrates at practical processing pressures and times was determined. Three experimental runs were made in which temperature was held constant at 275.4 K (36°F), and the surfactant concentration was maintained at 286 ppm; procedure and other conditions except pressure were repeated. Hydrates were formed in the cell until all of the water became tied up in the hydrate structure, i.e., interstitial water also formed hydrates. Individual runs were made at pressures of 3.89, 3.47, 3.11, 2.76 MPa (550.2, 503.6, 451.2, and 400.5 psig). The chosen pressure

was kept constant throughout the run with the constant pressure regulator, and the rate of gas occluded was measured with the gas mass-flow meter. Such a procedure gives a greater storage capacity than when pressure is allowed to drop and would be a preferred procedure in a large-scale process.

The storage capacity of the gas hydrates as a function of time after hydrate initiation is given in Fig. 17.

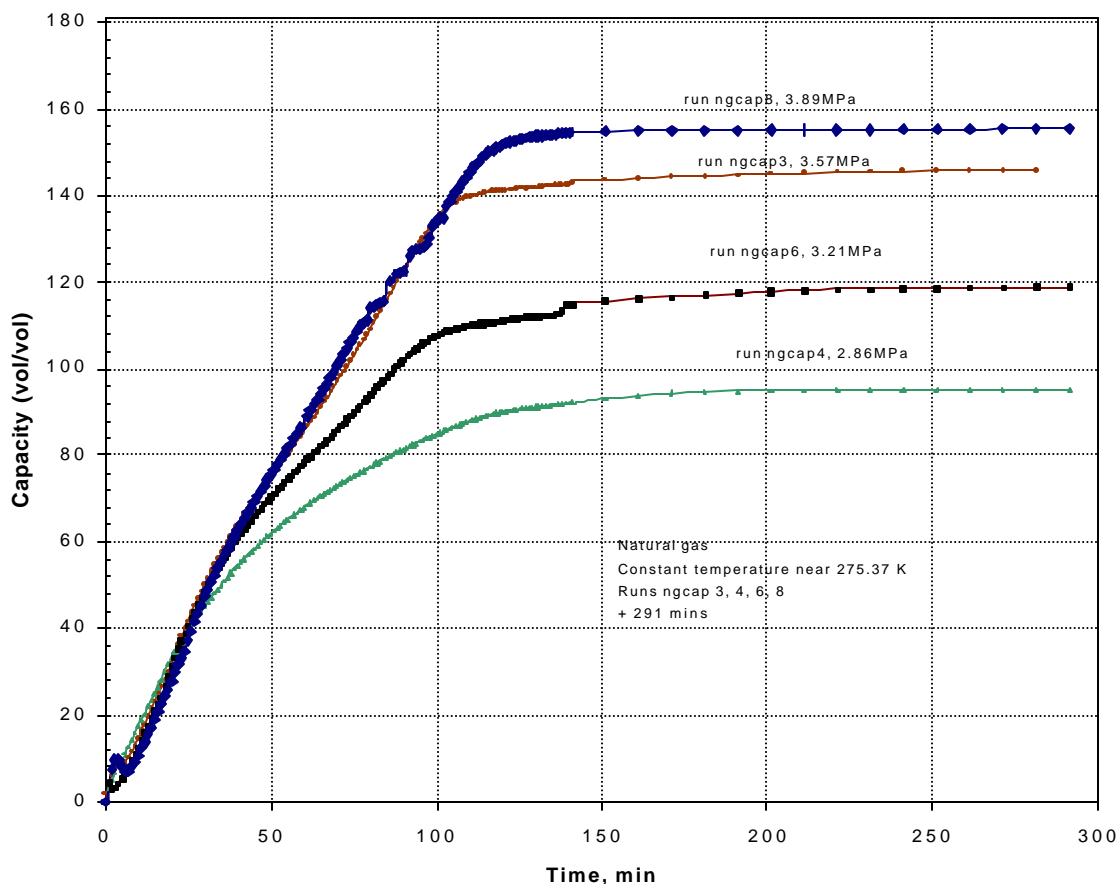


Fig. 17. Pressure increases natural gas storage capacity.

The results reflect an increase of storage capacity as pressure increases, since higher pressures cause more cavities in each crystal to be filled with gas and the interstitial water to be fully reacted.

These results show that 155 (vol gas)/(vol hydrate) storage capacity is achieved at a processing pressure of 3.89 MPa (564.9 psia). Furthermore, this much gas is incorporated into the hydrates in less than 3 hours of processing time. The 155 vol/vol represents 86% of the theoretical storage capacity if all cavities were filled. The results emphasize the technical feasibility of the process.

If a common time during formation is taken in Fig. 17, 291 minutes for example, the storage capacity is seen to increase with pressure as given in Fig. 18. At the 3.57 MPa (518 psia), a storage of 148.4

vol/vol is achieved; at 3.89 MPa (564.9 psia), a storage capacity of 155 vol/vol is achieved. One can anticipate that even higher pressures would improve capacity further, but the higher pressures would necessarily increase storage tank costs.

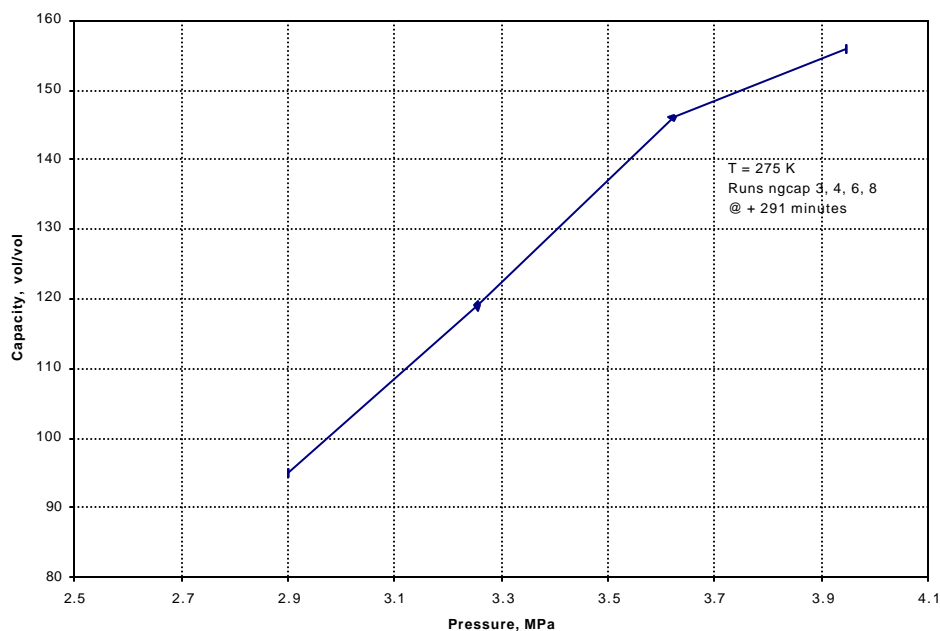


Fig. 18. Pressure trends of natural gas storage capacity.

From Equation (6) if surface tension, gas-water interfacial area, temperature, and degree of supercooling are kept constant, as in the runs of Fig. 18, then the equation reduces to

$$r = C P^{\tilde{a}} \quad (7)$$

where

$r$  = rate of hydrate formation

$C$  = a constant

$P$  = pressure

$\tilde{a}$  = overall order of reaction with respect to pressure

Therefore, as our data supports, the rate of hydrate formation is a function of pressure with the surfactant-water-natural gas system.

### III. Temperature Effects

A latent heat of formation of about 65.4 kJ/mol (Sloan, 1990) is released at the water-gas interface when hydrates form, introducing heat transfer rate as a factor in the formation rate as it affects the temperature terms in eq. (6). The relatively large release of heat creates an experimental problem of determining a true interfacial temperature. Stainless steel surfaces increase formation rates by their conductive removal of heat from the interface and facilitate formation by being a promoter of nucleation.

The release of latent heat during hydrate formation is illustrated in Fig. 19 as a comparison of liquid-phase and gas-phase temperatures in the laboratory test cell. In this run, cell and water contents at ambient temperature were pressurized with natural gas initially and then cooled to 277.1 K (39°F); pressure decreased according to the gas law until hydrates began forming whereupon pressure dropped precipitously. Note that the RTD probe in the gas phase is much more sensitive to the release of the latent heat in our laboratory test cell. It illustrates the difficulty of measuring a true interfacial temperature which would have a value somewhere between the two traces in the figure below.

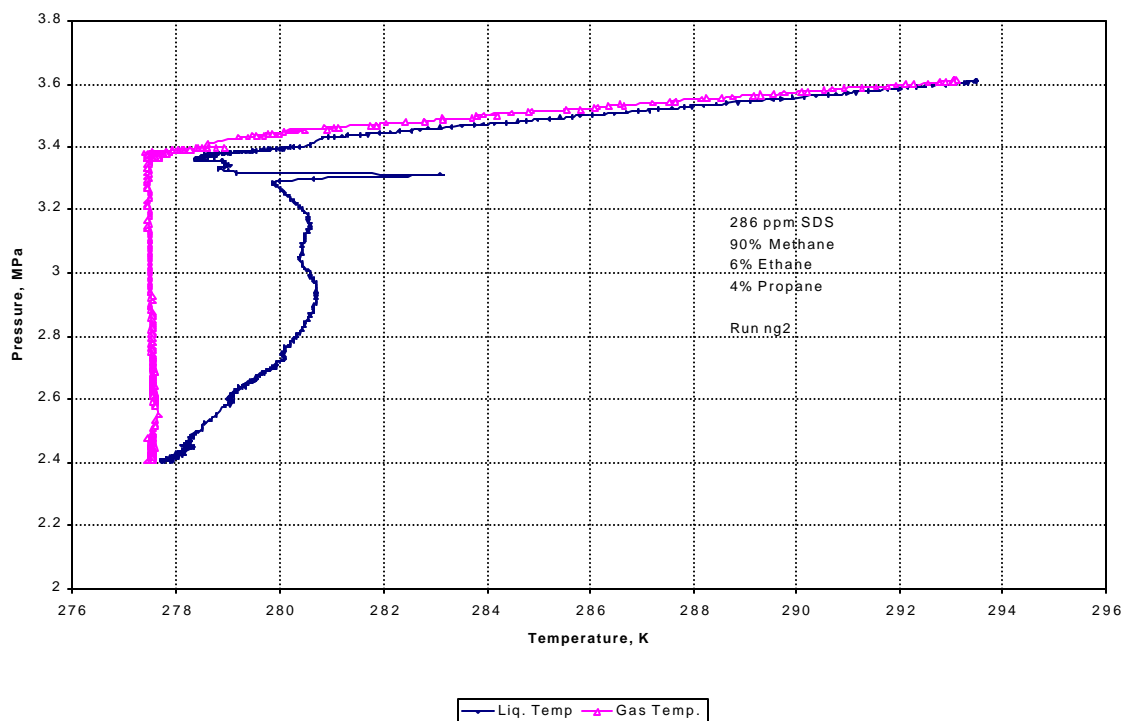


Fig. 19. Gas-phase temperature more sensitive to natural gas hydrate formation.

#### IV. Natural Gas Composition Effects

##### A. Formation Compositions

Of the hydrocarbon gases present in natural gases, only methane will fit into the smallest cavities of Type I and help stabilize the crystal. Propane is necessary to stabilize the Type II hydrate crystal, although methane will fit into all three sizes of cavities in Type I and Type II hydrates. Therefore, storage of natural gas must involve forming Type II hydrate crystals, which means having propane present, in order to perform the process at practical pressures.

For a given temperature, hydrates are formed at lowest pressures from propane and the pressure gets progressively higher in the order propane-ethane-methane. Then, it is to be expected that for a mixture of the three gases, occlusion would be preferentially in the order propane-ethane-methane. Table III illustrates this.

TABLE III. Summary of occluded and free gas compositions.

Load #	P (MPa)	T (°K)	Calculated Occluded Gas Composition %			GC Free Gas Measured %		
			CH <sub>4</sub>	C <sub>2</sub> H <sub>6</sub>	C <sub>3</sub> H <sub>8</sub>	CH <sub>4</sub>	C <sub>2</sub> H <sub>6</sub>	C <sub>3</sub> H <sub>8</sub>
1. Begin	3.51	293.1	68.3	3.5	28.2	90.01	5.99	4.00
1. End	2.30	277.6	80.7	5.6	13.3	98.1	1.7	0.2
2. Begin	3.37	282.1	65.5	3.4	31.1	94.0	4.0	2.0
2. End	2.67	276.8	81.2	4.5	14/3	98.6	1.2	0.2
3. Begin	3.34	278.8	66.5	3.7	29.8	95.6	3.1	1.3
3. End	2.88	276.9	87.3	3.8	9.0	99.1	0.8	0.1
4. Begin	3.34	279.6	76.9	3.7	19.3	98.2	1.4	0.4
4. End	3.14	277.5	86.6	5.0	8.4	98.8	1.1	0.1
5. Begin	3.34	278.7	79.1	3.7	17.2	98.5	1.2	0.3
5. End	3.22	277.7	86.7	5.0	8.3	98.8	1.1	0.1
6. Begin	3.34	278.4	82.2	4.4	13.4	98.6	1.2	0.2
6. End	3.16	277.4	87.4	3.76	8.86	99.1	0.8	0.1

The data in Table III was taken in six successive batch loadings of the gas mixture of 90.01% methane, 5.99% ethane, and 4.00% propane. As hydrates formed from an initial pressure of

about 3.34 MPa (485 psia), pressure in the test cell declined to near equilibrium, whereupon more gas of the original composition was added to bring the pressure back up to about 3.34 MPa. This was repeated five times. Free-gas compositions in the test cell were determined at the beginning and ending of each loading by gas chromatography; occluded-gas composition at equilibrium in the hydrates of the test cell were calculated by statistical thermodynamics (Sloan, 1992).

Note that the free gas in the test cell becomes progressively richer in methane; the free gas concentration of methane increases from 90.01% initially to 99.1% at the end of the sixth loading, whereas propane concentration in the free gas decreases from 4.00% to 0.10%. The first gas occluded in the hydrates contains 68.3% methane and the last hydrates formed have 87.4% methane. If withdrawal of gas with changing composition creates any difficulty in end-use, a surge-mixing tank could be installed on the outlet gas stream.

Some important applications to large-scale storage of natural gas in hydrates are derived from the data of Table III: (1) Lower storage/formation pressures of the natural gas will be realized with increasing propane and ethane concentrations in the natural gas. (2) If the free gas rich in methane were to be withdrawn from the formation vessel for some auxiliary use, substantially lower storage pressures would be realized. (3) Higher formation rates and greater storage capacity would be realized if feed gas were to be admitted to the hydrate tank at an initial pressure that remained constant in a semi-continuous process.

#### B. Withdrawal Compositions

The withdrawal gas composition will result from combining occluded gas released from hydrates and free gas above the hydrates. The occluded gas becomes leaner in methane as decomposition of the hydrates proceeds. In Table IV is summarized the composition as analyzed with the gas chromatograph of the withdrawn gas from the test cell at three stages of decomposition: start, midway, end. The changing composition reflects the scavenging effect of the hydrates for propane and ethane.

Again, if withdrawal of gas with changing composition creates a difficulty in end-use, a surge-mixing tank could be installed on the outlet gas stream.

TABLE IV. Natural gas withdrawal compositions.

<b>Component</b>	<b>Begin</b>	<b>Midway</b>	<b>End No Hydrates Remain</b>
<b>Methane</b>	99.1	94.1	76.5
<b>Ethane</b>	0.8	5.2	12.4
<b>Propane</b>	0.1	0.7	11.1
	458 psia 39.5 F	227.7 psia 38.6 F	207.1 psia 76.1 F

## V. Decomposition

### A. Hysteresis of Formation/Decomposition

Decomposition of the hydrates proceeds as rapidly as heat can be transferred to the solid mass for the latent heat of the phase change. In our test cell with the cooling/heating coils inside the cell in direct contact with the water and solids, decomposition rate was limited only by the capability to dispose of the liberated gases. Since the hydrocarbon gases removed from the cell in the laboratory were always mixed with nitrogen to a composition beyond the flammability limit, the hydrate decomposition rate was necessarily limited by our disposal rate. Therefore, the decomposition rate was studied by retaining liberated gases in the test cell and allowing cell pressure to rise. The decomposition rate is sufficient to meet process requirements under these conditions, although higher rates could be achieved if pressure was decreased and gases removed as would occur in a large-scale process. Also, the decomposition rate proved sufficient with a moderate temperature of 294.3 K (70°F) in the circulating water; therefore, in a large scale process a low-quality heat source could serve to decompose the 274.8-277.6 K (35-40°F) hydrate particles. For example, water from a power plant at 311 K (100°F) normally sent to a cooling tower to lower temperature for reuse would suffice.

In Fig. 20 is the formation and decomposition curves for ethane hydrates in a quiescent system of pure water-ethane. (No surfactant was present.) The pressurized system was cooled to form the hydrates and then allowed to decompose as pressures and temperatures were monitored.

Note that the equilibrium curve is superposed as the dotted line in Fig. 20.

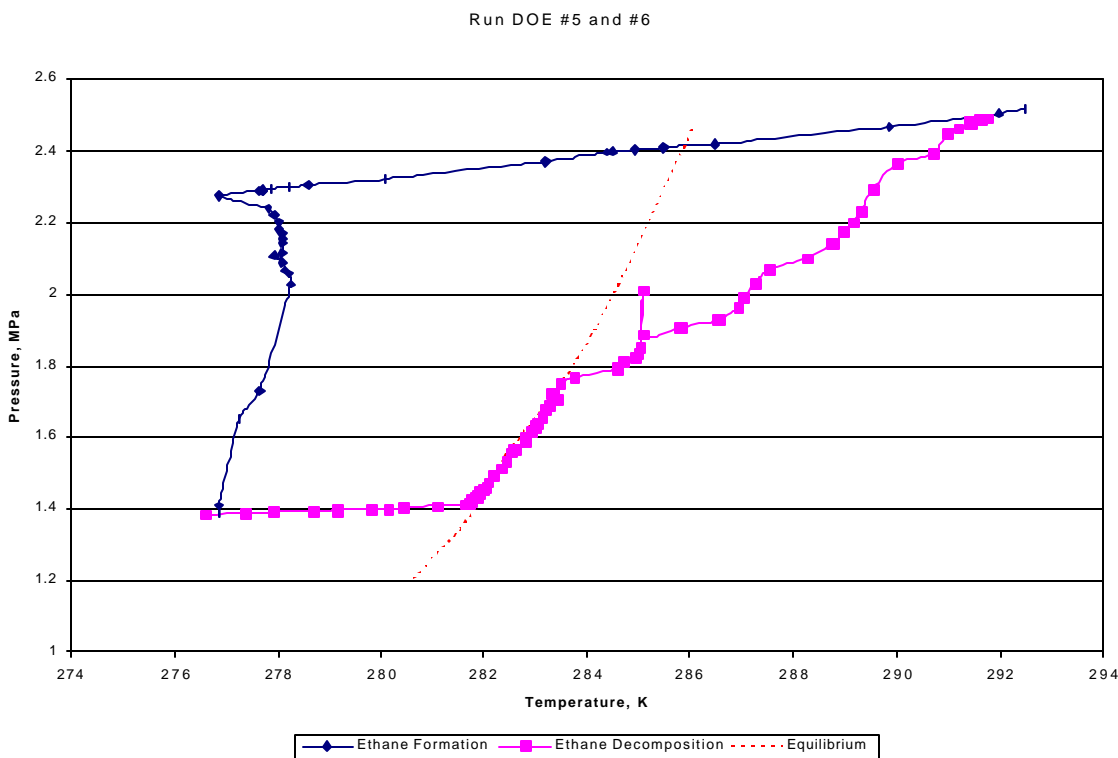


Fig. 20. Hysteresis of formation/decomposition cycle.

Note that as the temperature decreases below the equilibrium curve at about 285.4 K (54°F), a faster drop in pressure occurs as hydrate nuclei begin to form in the cell. The net effect as the nuclei form is an apparent increase in the solubility of ethane in water. After supercooling, hydrates particles formed and pressure dropped steeply. If formation had been allowed to continue past 1.38 Mpa (200 psia), the equilibrium curve eventually would have been approached. On adding heat to the system, the solid particles first warmed to near the equilibrium temperature without decomposition, decomposition followed the equilibrium curve, and then the system returned to the original temperature and pressure when all of the hydrates had been decomposed. The hysteresis observed in Fig. 20 is typical.

Afterwards, in another experimental run with SDS surfactant in the water, the cell was packed to near capacity with hydrates. Then, the hydrate decomposition inside the pressurized cell was captured on VHS video film. It is interesting that the gas evolved from the hydrates remained intact as bubbles as it moved through the gas above the hydrates. The movement of the bubbles appeared similar to gas bubbling through liquid water, although there was no free water present in the cell. An explanation is offered that the occluded gas is surrounded by the hydrogen-bonded-water-cage which has on its outer surface the surfactant excluded from the hydrate structure; possibly, upon decomposition the released gas expands to form a bubble with the released water-surfactant forming the boundary. The movement

of the bubbles is vividly seen on the video tape, although capturing a still photograph from the film for this report was only partially successful. Figure 21 is a camera photograph from the monitor while playing the film from a VCR.



Fig. 21. Photograph of gas bubbles during decomposition.  
(Photo from VHS film)

Installing a demister on the exit line of any storage tank during decomposition should be a simple solution to an implied problem of entrained water.

#### B. Effect of Total Pressure on Decomposition

After the hydrocarbon gases are occluded in the solid matrix of the hydrate, the stability can be maintained at that temperature as long as the total pressure is maintained at the equilibrium point, or higher. That is, an inert gas could be used to displace the free hydrocarbon gas and maintain the total pressure above the natural gas hydrate during storage, for example, in cases of long-term storage or when extreme precautions against tank leakage were desired during the storage period.

### C. Decomposition with Microwaves

Microwaves were investigated for decomposing hydrates. Pressure transducer and RTD probes were positioned in the test cell as in other tests of this report. It was necessary to have at least a 7.62 cm (3 in) diameter quartz transparent window through which to inject the microwaves. A 5.08 cm (2 in) thick quartz was necessary to contain up to 6.89 Mpa (1000 psi) gases in the test cell. An adapter was designed and fabricated to attach the quartz window on the top of the cell and seal it to prevent gas leakage at the high pressure. A 10.2 cm (4 in) i.d. aluminum elbow connected the cell to the microwave generator. The microwave generator was a Gerling Laboratories, Model GL 114 at an operating frequency of 2450 MHz. Microwave power can be adjusted up to 1500 watts; amount of energy reflected in the delivery train is monitored and the difference between generated and reflected power is that injected into the cell. A 1.83 m (6-ft) wire screen around the apparatus was used as added protection of personnel.

The tests were run before the discovery of the beneficial effects of surfactant upon hydrate formation rate, so that the hydrates prepared for the microwave tests had been slowly grown over a period of about 4 days and were present in a random mass of solid crystals above the water in the bottom of the cell as seen in Fig. 9. No free water was visibly exposed to microwaves; the hydrates gave a solid covering of the free water in the bottom of the cell.

In Fig. 22 is a sketch of the experimental setup.

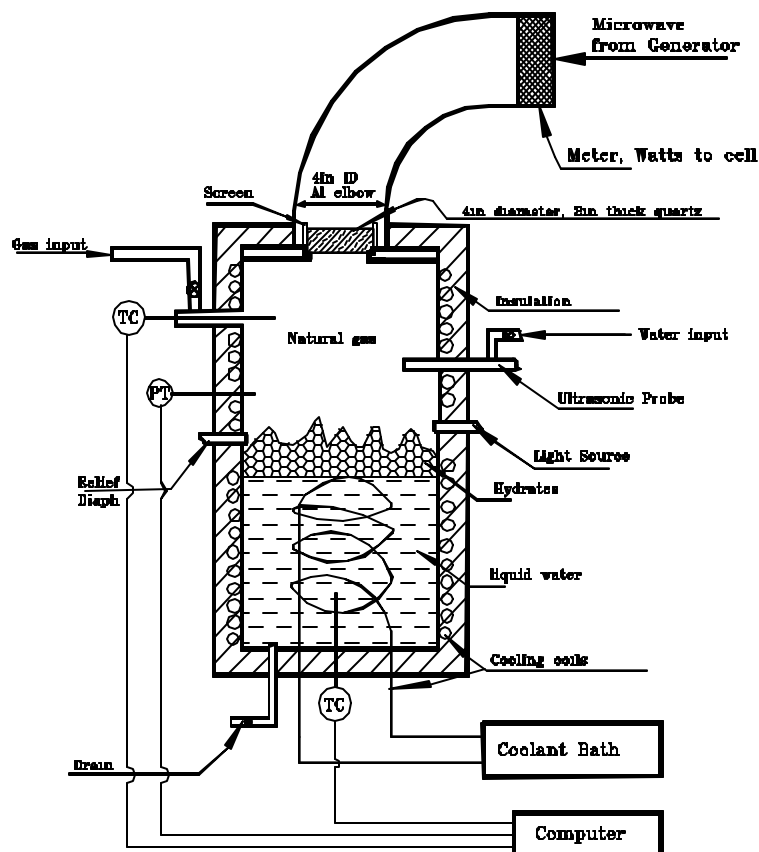


Fig. 22. Apparatus for microwave injection.

As indicated on the sketch of the apparatus, pressures and temperatures in the test cell were continuously recorded on the computer as the microwave tests were run.

A standard effect was established of microwaves on pure water in the cell pressurized to about 1.99 MPa (289 psi) with nitrogen chilled to 286.5 K (56° F). Microwaves were injected in 30-second pulses with 2 minutes between pulses. The schedule of microwave pulses was 100 watt increments from 60 to 860 watts. Pressure showed stepwise increases as microwave pulses vaporized some of the liquid.

Figure 23 shows the standard effect of microwaves.

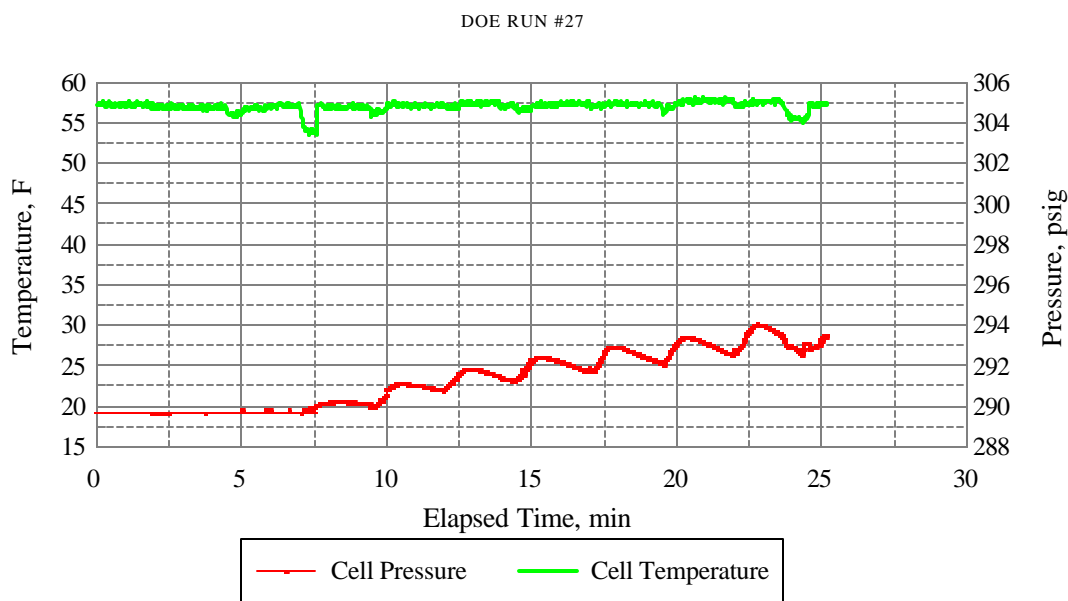


Fig. 23. Microwave response with water in system.

From a similar schedule of microwave pulses into the cell containing hydrates at 1.99 MPa (289 psi) and 285.4 K (54° F), resulting temperatures and pressures are presented in Fig. 24. Note that steeper pressure steps resulted and pressure spikes formed on each microwave input. One surmises that additional gases were evolved as well as hydrate-structure-water being vaporized, i.e., hydrates were dissociated. Water associated with the hydrate matrix would have also vaporized to give similar peaks to the liquid water standard. Again, the liquid water in the bottom of the cell was covered by the mass of hydrates and not irradiated.

Also note in Fig. 24 some difference in the gas temperature behavior. At about 190 watts of microwave input, positive temperature spikes occurred upon injection, whereas at lower wattage negative spikes resulted. It is speculated that excessive energy entered the cell above 190 watts to be dissipated in the gas phase.

Note that the peaks in Fig. 24 include water from the hydrate structure and gas released from the hydrate structure.

DOE RUN #22

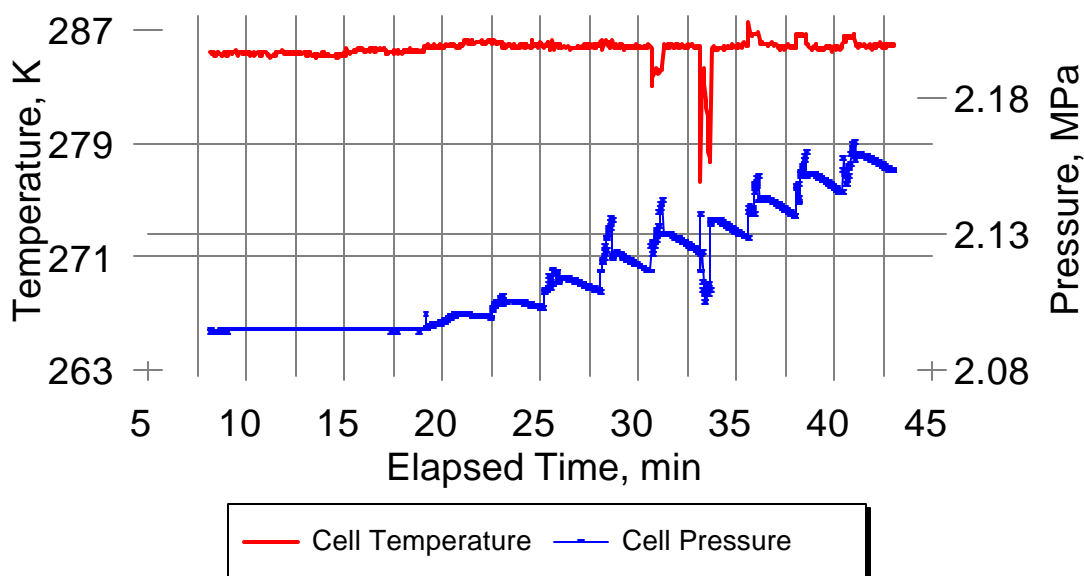


Fig. 24. Hydrate decomposition with cascading microwave pulses.

Input wattage of the microwaves was increased stepwise. Results are given in Fig. 25.

The gas released from hydrates as a function of power input was than calculated.

An optimum wattage seemed to exist as given in Fig. 25. Above the 190 watts, gas liberated per watt decreased.

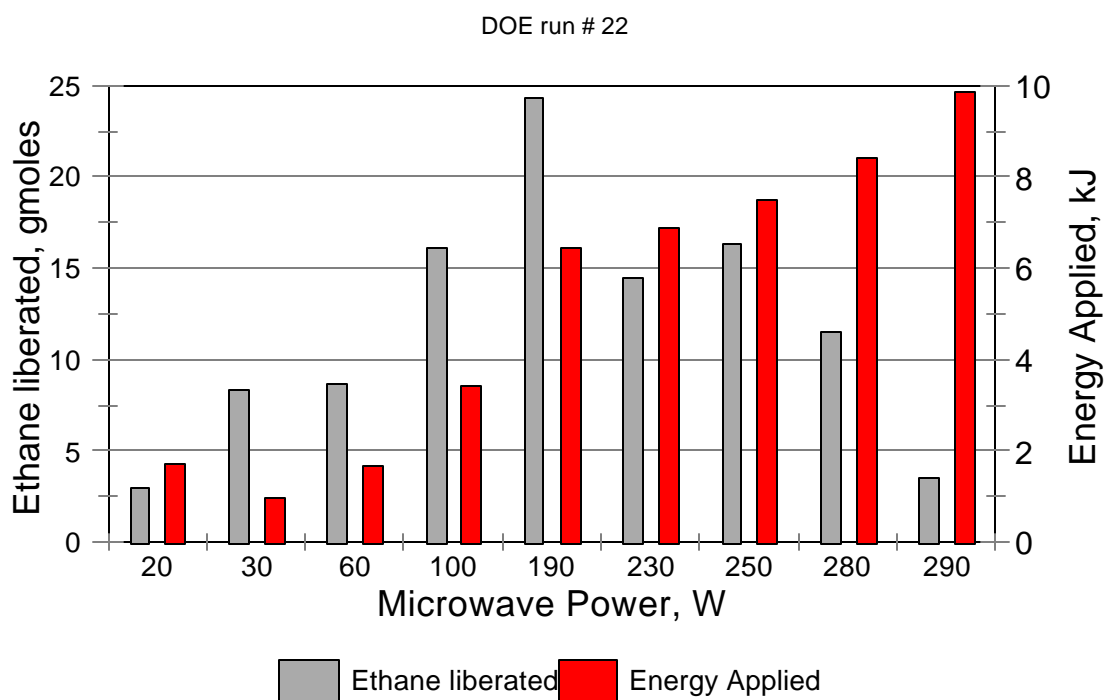


Fig. 25. Optimum microwave wattage for hydrate decomposition

The microwave experiments were not continued because decomposition of hydrates in a large scale process could be achieved very cheaply, especially near a power plant, with low-grade water of 376.5 K (110 F) or cooler that would ordinarily be sent to a cooling tower, anyhow. However, the results are kept in mind for possible specialty applications in this process.

## VI. Impact of Study on Hydrate Storage Feasibility

### A. Statement of Process Technical Need and Capability

The feasibility of gas hydrates for storing natural gas was studied because of their potential storage capacity of 180+ vol/vol and their inherent safety of essentially gas encased in ice at relatively low pressures. Furthermore, large quantities of natural gas are known to be stored this way naturally in ocean sediments and arctic regions.

Since hydrates have never been used for the industrial storage of gas, the feasibility study began with some major questions about such a process involving gas hydrates. Could the hydrates be formed rapidly enough? Prior to this study, formation of hydrates was a slow process in the laboratory, especially if using the simplest of systems--quiescent water and gas. Although hydrate formation had been shown by numerous people before the study to be rapid if mechanical stirring was used in the laboratory, a mechanically-stirred system under pressure at low temperatures on a large scale would not be practical from the standpoint of maintenance, initial equipment costs, labor, and leakage. Another question was whether a high bulk density of the hydrates could be realized? Or could a process step to collect the hydrate crystals from the water and pack them be practical? These were imposing questions, for water was known to be trapped inefficiently between solid hydrate particles and made inaccessible to further hydrate formation in previous laboratory work. In a scale-up, because of tank size and cost, one could not tolerate approximately 80% of the storage space to be occupied by unreacted water, as had been reported. Finally, could the process be made simple enough to be practical and economical?

A breakthrough occurred early in the work that provided answers to the preceding questions. By using the surfactant sodium dodecyl sulfate in concentrations as low as 286 ppm in water, the desired properties are achieved: (1) Hydrates form rapidly--about 700 times faster than without surfactant. (2) Free water trapped between particles is fully utilized to give a high bulk density. (3) Particles move from the water solution as they form and deposit (pack) on the chamber walls. (4) Hydrates form in a simple quiescent system. (5) 86% of the theoretical storage capacity can be achieved within 3 hours of hydrate initiation. (6) 155 vol-gas/vol-hydrate can be stored at 3.89 Mpa (564.9 psia) and 275.4 K (36°F).

These experimental observations suggest ideas for a practical design for large-scale natural gas storage in hydrates.

### B. Hydrate Formation/Storage Tank

#### *(1) Characteristics to incorporate.*

The interpretation of the laboratory observations relate to a design concept for a hydrate formation/storage/ decomposition tank as follows.

1. A single tank would serve for forming the hydrates as well as storing and decomposing them. This would negate the need for a tricky process step of pumping a cold liquid slurry of water-hydrate particles under pressure.
2. The hydrate particles form subsurface in water when it contains surfactant. This allows the formation process to proceed with a stagnant, unstirred water-surfactant solution. The many attendant problems of mechanical agitation of a thickening slurry under pressure are avoided. One would only admit more gas to the tank as it is occluded into the hydrates.
3. The hydrate particles move from the surfactant solution as they form and pack on the tank walls because of the adsorption of surfactant on the walls. This means no separation steps to remove hydrate particles from the water and pack them for storage is necessary. The particles pack into a desired arrangement as they form.
4. The free water trapped between hydrate particles on the tank walls continues to form hydrates because surfactant is excluded from the hydrate structure and transferred to the surrounding water. In fact, the rate of formation increases because of the greater surface area as more hydrates form--up to the point where a decreasing permeability slows the rate. Therefore, a high bulk density is achieved in the packing.
5. The rate of formation is high with surfactant present in the water. Our laboratory data indicate 86% of theoretical storage capacity is achieved within 3 hours after hydrate initiation. Moreover, this rate occurs in a quiescent system. The high rate indicates that a complete formation-decomposition cycle with adequate turnaround time could be achieved well within a 24- hour period at a very low labor requirement.
6. Water-surfactant solution wets the walls of the storage vessel. As particles collect on the walls, the water level drops, so that at the end when the last free water is in the cell, the hydrate mass is above the free water in the cell bottom.
7. Decomposition could be realized with heat transfer from a relatively low-temperature medium.
8. A substantial latent heat must be accommodated in the phase change.

(1) *Sketch of tank concept.*

The following Fig. 26 of a concept of a hydrate formation/storage/decomposition tank is suggested. (Zhong, et al., 1998)

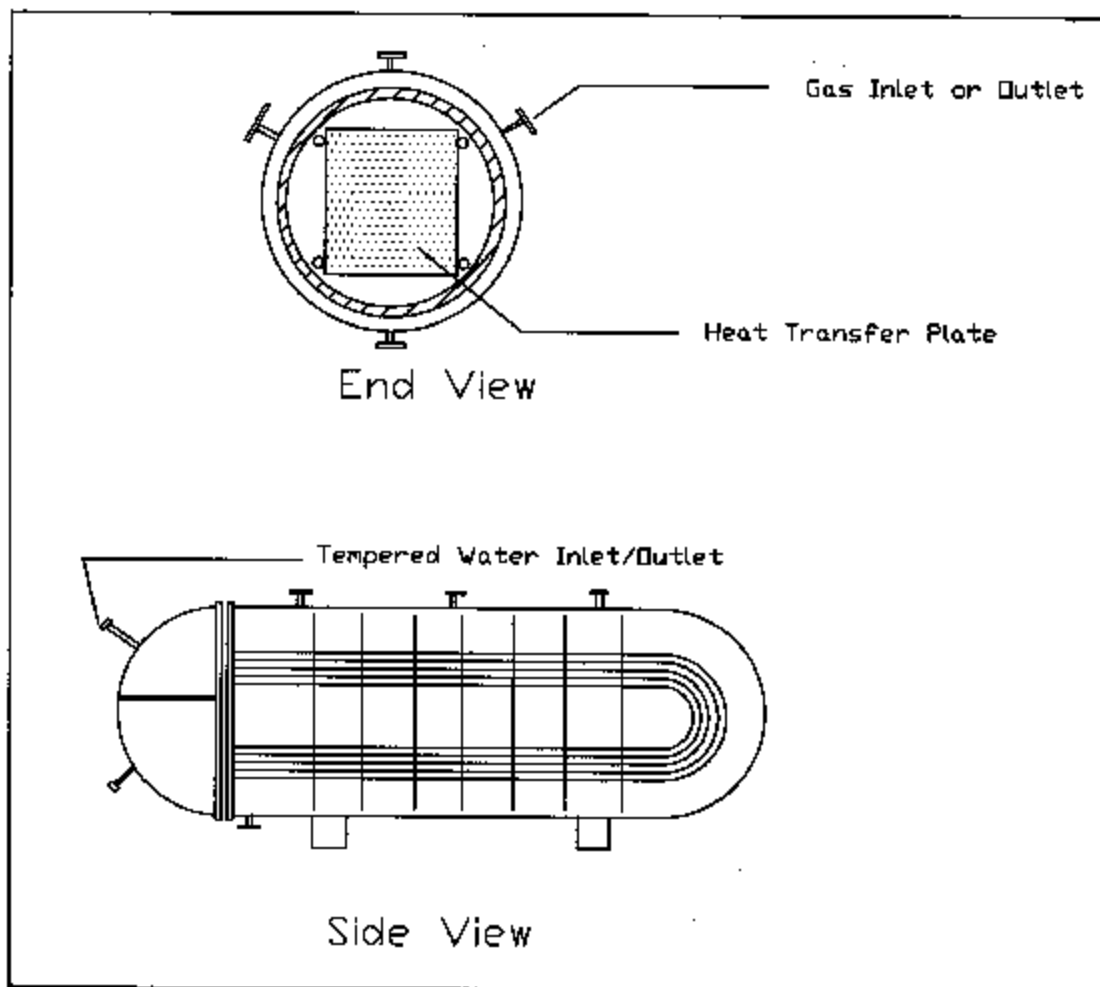


Fig. 26. Hydrate formation/storage/decomposition tank (Zhong, Montgomery, Pitman, Bounds).

To incorporate the findings of the laboratory test cell, the storage tank for an industrial-size facility features 9 thin stainless-steel plates 0.813 mm (0.032" thick) attached as a unit to tubing for a closed-loop flow of cooling or heating fluid, depending upon whether a formation or decomposition step is in progress. The plates and tubing are suspended on a rack that can be pulled as a unit from the horizontal tank for maintenance.

During hydrate formation, cooling fluid would circulate through the tubing to remove latent heat of hydrate formation. Heat transfer would be by conduction from direct contact of tubing with

plate and by conduction-convection to the water surrounding the tubing and plates. Gas would be admitted or withdrawn through the top ports. Gas hydrates would form on both sides of all plates and on the inside walls of the tank. The nine plates and inside surface area of the tank give an equivalent volume-surface ratio as was present in the laboratory test cell.

A time sequence depicting hydrate formation on the heat-transfer plates of the tank is given in Fig. 27.

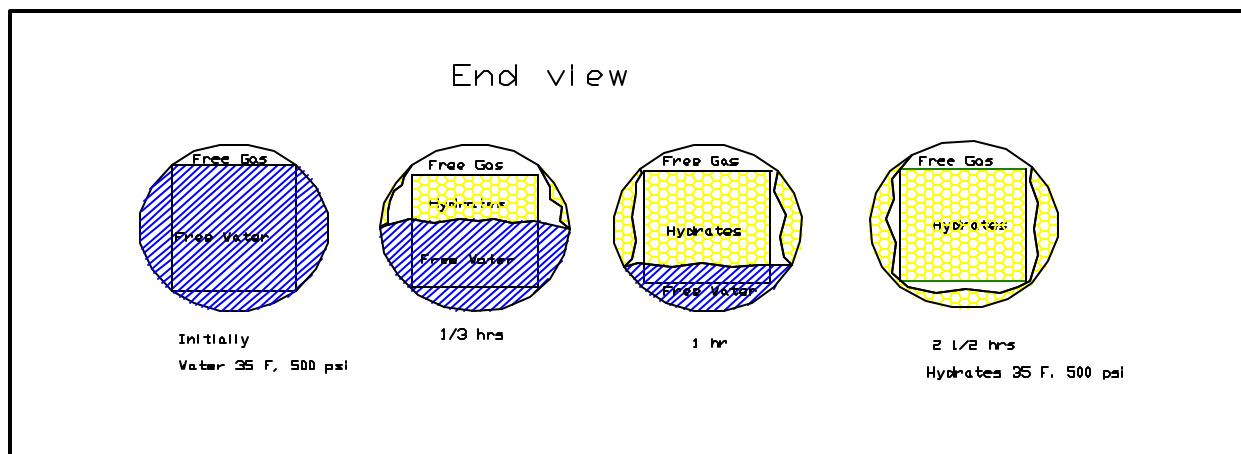


Fig. 27. Time sequence of hydrate formation in storage tank.

Water-surfactant are envisioned as initially submerging the plates. Free gas at 3.89 Mpa (564.9 psia) is admitted continuously. Hydrate forms on all the metal surfaces and the water level drops. Gas is replenished to maintain initial pressure. All of the free water is tied up by the fourth frame. Gas continues to form hydrates from trapped interstitial water until 86% of the theoretical gas capacity of hydrate storage is reached in about 2 ½ - 3 hours.

Decomposition is a reversal of these steps as warm water is passed through the heat-transfer coils.

In Fig. 28 is a side-view depiction of how hydrate particles would build on the inside surfaces of the formation tank and plates.

The sketch is based on observations of the particle build up in the laboratory test cell.

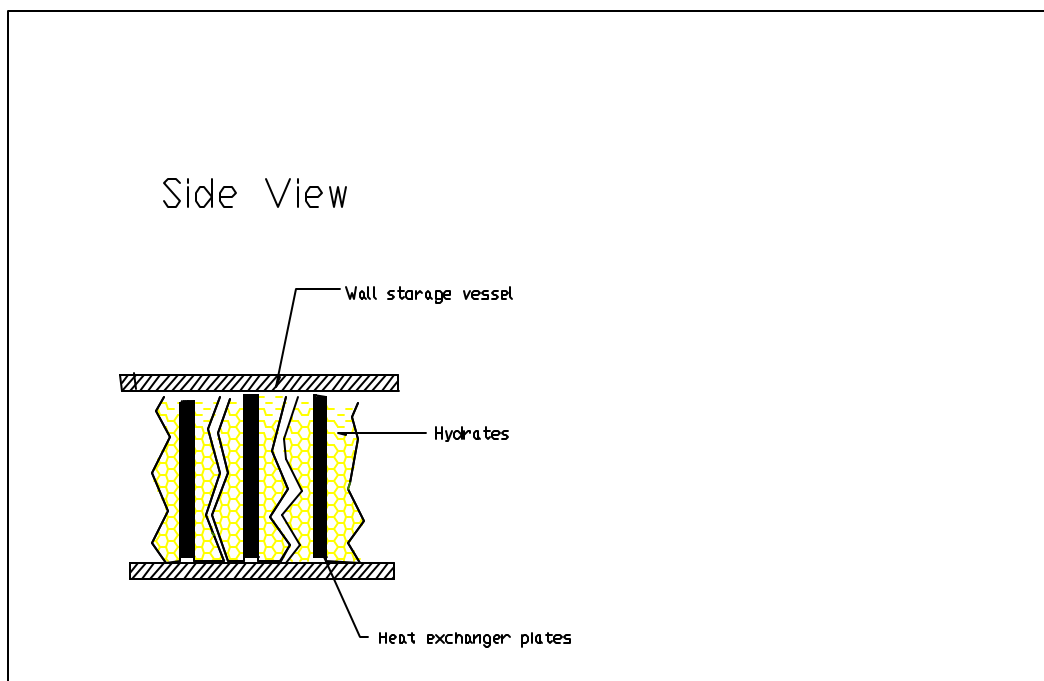


Fig. 28. Concept of hydrate accumulation in storage tank.

These ideas for a storage tank design would be pursued in the follow-on study to establish a final design and determine the economics of a large-scale hydrate storage process.

## VII. CONCLUSIONS

The following major conclusions pertaining to the feasibility of storing natural gas in gas hydrates are made as a result of studies under the contract DE-AC26-97FT33203.

1. It is technically feasible to store natural gas in hydrates on a scale for industrial applications.
2. At a pressure of 3.89 Mpa (550 psig) and a temperature of 276.0 K (37°F), 155 (volume gas at standard temperature and pressure)/(volume hydrate) can be stored from a feed gas typified by 90% methane, 6% ethane, and 4% propane.
3. Concentrations of surfactant in the water above the critical micellar concentration (242 ppm) enhances process feasibility greatly:
  - A. Increases formation rate of the hydrates by a factor of about 700.
  - B. Causes the hydrate particles to adsorb on the tank walls as the hydrate forms, thus eliminating the need for separation of particles from the cold water-hydrate slurry.
  - C. Maximizes gas content of the packed hydrate particles, as trapped free water between packed particles continues to form hydrates after adsorption on the vessel wall until complete utilization of trapped water is approached.
  - D. Simplifies process. Allows a quiescent system to form hydrates.
  - E. The surfactant is cheap; small amounts are required; it is nontoxic, biodegradable.
4. The rate of hydrate decomposition can be controlled by the heat transfer rate to the hydrate particles. An ambient temperature heating medium can be used to give an adequate decomposition rate.
5. Propane concentrations of at least 1- 4% must exist in the feed gas along with the methane in order to adequately store gas below 3.89 Mpa (550 psig) as Type II hydrates. As ethane and propane concentrations in the feed gas are increased, required formation and storage pressures decrease.
6. Occluded gas composition depends on feed gas composition.
7. A storage tank design can be devised from knowledge of the experimental results.

## **VIII. RECOMMENDATIONS**

The use of surfactants makes a process for storing natural gas in hydrates technically feasible. The next step should be to develop a design for a large-scale process based on the laboratory results. In conjunction with the design, an economic study should be made estimating total capital investment, production costs, and storage costs per volume of gas per cycle over the life of the facility.

## BIBLIOGRAPHY

Carson, B.D., and Katz, L.D., "Natural Gas Hydrates," *AIMME Tech. Pub.* No. 1371 (1941).

Englezos, P., "Nucleation and Growth of Gas Hydrate Crystals in Relation to 'Kinetic Inhibition'", *2nd International Symposium on Gas Hydrates*, Toulouse (1996) 147-153.

Herri, J., Gruy, F., and Cournil, M., "Kinetics of Methane Hydrate Formation," *2nd International Symposium on Gas Hydrates*, Toulouse (1966) 243-250.

MacKerrell, A.D., Jr., "Molecular Dynamics Simulation Analysis of a Sodium Dodecyl Sulfate Micelle in Aqueous Solution: Decreased Fluidity of the Micelle Hydrocarbon Interior," *J. of Phys. Chem.*, **99** (1995) 1846-1855.

Makogon, Y.F., *Hydrates of Natural Gas*, PennWell Books (1981).

Marita, H., and Uchida, T., "Studies on Formation/Dissociation Rates of Methane Hydrates," *2nd International Symposium on Gas Hydrates*, Toulouse (1996) 191-197.

Mori, Y., and Mochizuki, T., "Modeling of Mass Transport across a Hydrate Layer Intervening between Liquid Water and 'Guest' Fluid Phases," *2nd International Symposium on Gas Hydrates*, Toulouse (1996) 267-274.

Sloan, D.E., Jr., *Clathrate Hydrates of Natural Gases*, Marcel Dekker Inc., New York, NY, (1990).

Sloan, D.E., Jr., "Natural Gas Hydrates," *J. Petroleum Technology*, **43**, No. 12 (1991) 1414-1417.

Spontak, R.J., "Determination of Volumetric Properties for Systems Containing Structure I Gas Hydrates," *Industrial Engineering and Chemistry Process Design Development*, **25**, No. 4 (1986) 1030-33.

Tse, J.S., et al., "Molecular Dynamics Studies of Ice and Structure I Clathrate Hydrate of Methane," *J. of Physics and Chem.*, **87** (1983) 4198-4203.

Vysniauskas, A., and Bishnoi, P.R., "Kinetics of Ethane Hydrate Formation," *Chemical Engineering Science*, **40** (1985) 299-303.

Vysniauskas, A., and Bishnoi, P.R., "A Kinetic Study of Methane Hydrate Formation," *Chemical Engineering Science*, **38** (1983) 1061-1072.

Wilcox, W.I., Carson, D.B., and Katz, D.L., "Natural Gas Hydrates," *Industrial and Engineering Chem*, **33**, No. 5 (1941) 662-65.

Zhong, Y., Montgomery, R., Pitman, R. And Bounds, M., *Plant Design*, Senior chemical engineering project assignment, Mississippi State U., Dept. of Ch.E., Nov. 1998.

## LIST OF ACRONYMS AND ABBREVIATIONS

SDS	The anionic surfactant sodium dodecyl sulfate.
CMC	The critical micellar concentration. A threshold of surfactant concentration in water solution, at which point many physical properties abruptly change.
RTD	Resistance temperature detector.